

Pharmaceutical Emulsions and Suspensions

edited by
Françoise Nielloud
Gilberte Marti-Mestres

*Laboratoire de Technique Pharmaceutique Industrielle
Université Montpellier I
Montpellier, France*



MARCEL DEKKER, INC.

NEW YORK – BASEL

2000

This is a fac-simile of the last draft of a book chapter. You are intitled to consult this pdf version if your institution owns the book or if your are following a course taught by the author of this chapter.

3

Emulsion Properties and Related Know-how to Attain Them

Jean-Louis Salager

*Lab. FIRP, Chemical Engineering School,
University of the Andes, Mérida, Venezuela*

I. Emulsion Characteristics and Properties	74
A. Conductivity and Type	74
B. Drop Size	76
C. Stability	80
D. Emulsion Viscosity	92
II. Influence of Formulation on Emulsion Properties	98
A. Conductivity-Emulsion Type Change	98
B. Emulsion Stability	100
C. Viscosity	102
D. Drop Size	103
III. Formulation/Composition Map	104
A. Crossed Effects on Bidimensional Map	104
B. Conductivity Map and Emulsion Type	105
C. Stability Map	108
D. Viscosity Map	110
E. Drop Size Map	111
F. Effect of Other Variables on the Inversion Line	111
IV. Dynamic Phenomena in Emulsion Modification	115
A. Modifying Emulsions Without Inversion	115
B. Emulsion Dynamic Inversions and Applications	117

Acknowledgments	121
References	122

This chapter deals with emulsion properties, i. e., type, drop size, stability and viscosity. It shows how to estimate or measure them in practice, and how they are related to formulation, composition and other variables. The current know-how is presented in a comprehensive way so that the emulsion maker can use it to attain some suitable property. The case of emulsion made from preequilibrated surfactant-oil-water systems is treated first. Then follows a discussion on how to modify emulsions to seek specific properties, which leads to the introduction of the dynamic inversion phenomena, discussed from the practitioner's point of view.

I. EMULSION CHARACTERISTICS AND PROPERTIES

A. Conductivity and Type

Maybe the first and most important emulsion property to be determined is its type, i. e., either oil-in-water O/W or water-in-oil W/O, and eventually the occurrence of a multiple emulsion. This is essentially equivalent to determine which is the emulsion external phase.

There are different methods to do so. Since the external phase is the one that first touches whatever is in contact with the emulsion, the external phase and the emulsion exhibit similar wettability and dispersion properties. For instance, a dash of O/W emulsion would extend on a hydrophilic substrate like a clean glass slab or a filter paper, while an W/O would not. If a small amount of an O/W emulsion is poured in an aqueous medium its external phase would dissolve in the aqueous phase and its oil droplets would disperse. On the contrary, a W/O emulsion globule would not do so (1).

These are simple qualitative methods that only require the withdrawal of a small sample, but they are not amenable to in line or in situ measurement, such as to continuously monitor the emulsion type and to detect inversion occurrence.

In most cases the aqueous phase contains some electrolyte while the oil phase does not, so that the electrolytic conductivity is the property that is measured to detect the emulsion type.

As a first approximation it may be said that the electrolytic conductivity of an emulsion σ_{em} is proportional to the conductivity of its external phase σ_{ext} and to its volumetric proportion ϕ_{ext} .

$$\sigma_{em} = \sigma_{ext} \phi_{ext} \quad [1]$$

Actually the variation depends upon the drop size average and distribution, but it is not very sensitive, unless there are large changes in these characteristics. This means that the conductivity of an emulsion typically varies vs. the external phase proportion as indicated in figure 1 (left). The variation is proportional while it is an O/W type and it is essentially nil (at the same scale) when it is a W/O emulsion, because the typical electrolytic conductivity of the oil phase is 100 or 1000 times smaller than the conductivity of the aqueous brine. Consequently, the point where the emulsion switches type corresponds to a very large change in conductivity that may be detected even with a very rugged apparatus. The only requirement is to make sure that there is enough mixing so that the emulsion does not separate inside the conductivity cell. This is why conductivity cells that have a bell type anti-shock protector are inappropriate for this purpose since the dispersed phase drops are likely to settle in the unstirred zone and to fill it. The best suitable shape is an open geometry, eventually with a non conductor bridge between the electrodes as a reinforcement.

If an accurate conductimeter apparatus is used, a deviation from the straight line law may indicate the occurrence of a multiple emulsion. Consider for instance a $W_1/O/W_2$ type multiple emulsion with the proportions ϕ_1 and ϕ_2 of most internal (W_1) and most external (W_2) water phases respectively. If the total aqueous phase (proportion ϕ_{TW}) were located in the external phase the conductivity would be:

$$\sigma_{emT} = \sigma_2 (\phi_1 + \phi_2) = \sigma_2 \phi_{TW} \tag{2}$$

However the real external phase that conduces the electrical current is W_2 so that:

$$\sigma_{emR} = \sigma_2 \phi_2 \tag{3}$$

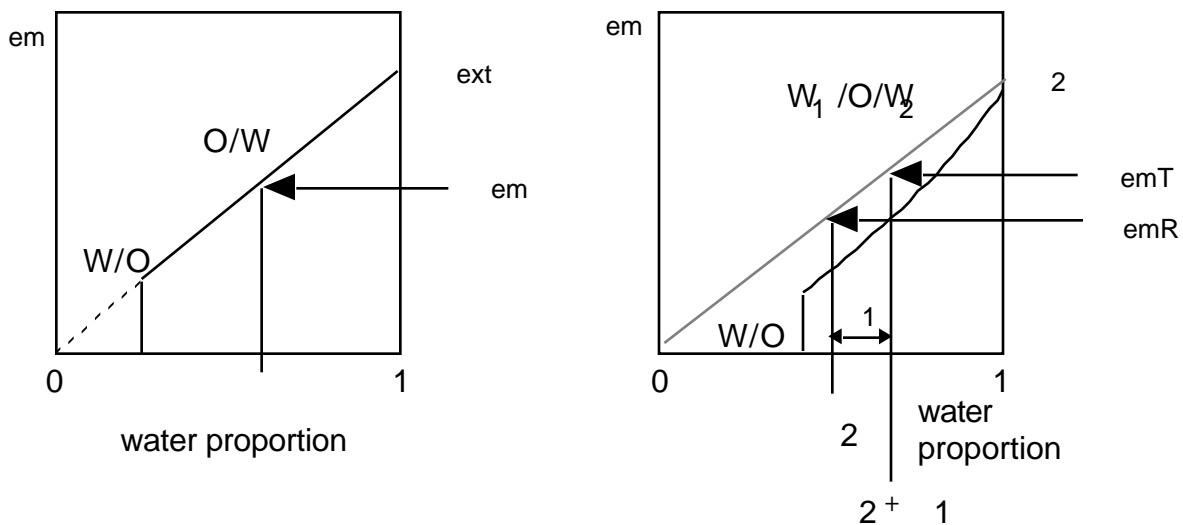


Figure 1: Variation of emulsion conductivity as a function of the water fraction, for a $SAD < 0$ (respectively $SAD > 0$) formulation at left (respectively right). (After reference 2)

which is the same expression as the previous one, but shifted toward a smaller value of the water phase proportion (see Fig. 1 right), the shift being the proportion of water ϕ_1 which is inside the oil drops (2).

$$\phi_1 = \phi_{TW} - \frac{emR}{2} \quad [4]$$

The presence of a multiple emulsion can be detected by conductimetry when ϕ_1 is about 2%, whereas it can be measured when it is more than 5%.

The application of multiple emulsion to controlled release or controlled transfer involves non equilibrium effects in which the most internal and most external phases, e. g. W_1 and W_2 in the previous case, have different compositions, so that a water transfer would take place under the osmotic pressure gradient.

In such a situation special care is advisable since the water transfer would change the external phase proportion ϕ_2 , as well as its electrolyte concentration c_2 . If the most inside droplets (W_1) contain a higher electrolyte concentration, water would be transferred from outside water (W_2) to inside water (W_1), i.e., ϕ_2 would decrease, while the electrolyte concentration in W_2 would increase, as well as c_2 . These opposite effects on the emulsion conductivity would make it quite insensitive to the mass transfer occurrence, and another detection method would have to be found.

B. Drop Size

After characterizing the emulsion type, the second most crucial information is the size of its drops. Since emulsification is generally a more or less random stirring process in which the breaking and coalescence steps are in dynamic equilibrium, the resulting emulsion is a polydispersed system in which small and big drops coexist. The outcome of this equilibrium depends upon a large number of factors that can influence the two antagonistic steps. Generally speaking, a lower tension or an increase in stirring energy and duration are expected to increase the break up, while a higher fluid viscosity would slow it down, and temperature would increase the coalescence rate (3-7). These statement may be true or false however, because in many cases a single variable can have opposite effects, as for instance the case of formulation and temperature which will be discussed in detail later on. It is thus safe not to make too straightforward guesses.

The best description of an emulsion is through its drop size distribution which gives a statistical inventory of the dispersed phase fragmentation. This information is extremely valuable in practice, because both the stability and viscosity depend upon the drop size distribution.

The drop size can be measured by several techniques from rugged to sophisticated and from cheap to expensive (8-9). The first type of method deals with the determination of an average

property linked to the dispersion size such as turbidity or reflectance. The problem is that they also depend upon the proportion of dispersed phase and other factors like the used wavelength and the refractive indexes. As a consequence, turbidity measurements in the so-called nephelometry technique are no longer used in practice, but in visual guessed diagnostics, which by the way could turn out to be pretty accurate if the observer is experimented. In effect it is known that the maximum turbidity is attained when the drop size is in the 2-5 μm range, and that it decreases whether the drops become smaller or larger.

The interaction between light and matter is a complex phenomenology that has been theoretically solved a long time ago, but has been applied to wide range instrumentation techniques only very recently, because of computational problems that could not be solved quickly before the arrival of digital computers.

The individual drop by drop analysis started with microscopic observation several decades ago. The method is tedious, and sometimes erroneous, for instance when big drops are flattened in between glass slides, or when the field depth is so small that the adjustment of the image plane cuts the drop above or below its equator, resulting in an apparent smaller size. These problems were not amenable to ready solution with the arrival of shape recognition software in the eighties.

Orifice obscuration methods have been used for about two decades as the first automated counting techniques. In these methods the diluted emulsion is forced to flow through an orifice or a short capillary, by a pressure gradient. When a drop passes through the orifice, a conductivity property is altered by the obstruction produced by the drop. It may be electrical conductivity between two electrodes placed on the two sides of the orifice, or light transmission through the orifice from a source to a photodetector. In both cases the obscuration of the property signal is translated to a drop size information by an appropriate data processing device. If the emulsion is diluted enough, the drops cross the orifice one by one so that an effective counting can be carried out and registered. After counting about 500 drops a statistical analysis can be carried out. These methods were, however, limited by the accuracy in detecting small drops, i. e., smaller than 10% of the orifice diameter, and by the eventual plugging of the orifice by big drops that could not pass through. As a matter of fact the range is typically 0.1 to 0.8 time the orifice diameter and a change of orifice is often necessary to accommodate different ranges. If the emulsion is very polydispersed, measurements with two or more different orifices are required to be matched to cover the whole the statistical distribution - a risky exercise as far as accuracy and reliability are concerned.

In the past ten years, the laser light scattering analyzer has displaced every other equipment, whenever the high price tag of this apparatus is no limitation. The method is based on the matter-light interaction according to Mie's law. In the usual macroemulsion drop size range, the diffraction angle increases as the drop size decreases, and the relation, although complex, is well known. Laser light pulses are sent at a quick pace through a cell in which a diluted emulsion quickly flows to get a

rapid renewal of the sample. With an expanded laser beam several drops can be intercepted simultaneously, with essentially no limit in size. On the other side of the cell an optical system measures the diffracted light at various angles at the same quick pace. Under these conditions only a few seconds are necessary to capture the signal from thousands of drops, a number that insures a high statistical significance. Thanks to improved optics and with the help of the computational muscle attained by personal computers, the light scattering signals can be translated into wide range drop size statistics in a very few seconds.

In a near future acoustic wave absorption might provide a way to estimate the drop size in opaque high internal phase ratio emulsions without dilution. However, the technique is still on probation.

Figure 2 indicates different types of distribution found in emulsions: unimodal of the log-normal type produced by turbulent homogeneous stirring; narrowly shaped or highly polydispersed; bimodal emulsions resulting from a mixture of two emulsions, which by the way might be intentionally made to attain a low viscosity.

The distribution frequency coming from the analyzer is generally in volume, i. e., the proportion of drops included into a class is the volume proportion of these drops with respect to the whole internal phase volume. In some cases the distribution in number or in surface is also required. It is worth remarking that if the distribution follows a log-normal statistics as it is often the case, the Hatch-Choate relationships may be used to readily translate volume distribution frequencies into equivalent number or surface distribution frequencies.

The notion of average size or distribution central tendency is a tricky one since there are many ways to calculate the mean, which are not at all equivalent, particularly with asymmetrical distributions.

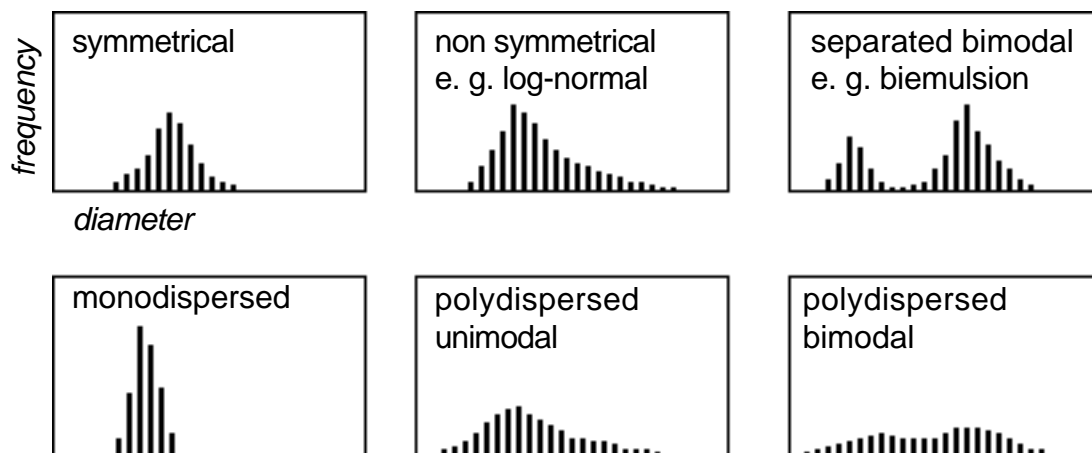


Figure 2: Different shapes of the drop size distribution

The mode is the most frequent size, while the median is the size so that half the internal phase volume is fragmented in smaller drops, and half in larger ones. It is often symbolized as $D(1/2)$ or $D(v,0.5)$.

Other used mean values are the mean of the distribution in volume or mass, so-called $D(4,3)$ because it is the ratio of the fourth moment of the distribution in number to the third one, or the mean of the distribution in surface, so-called Sauter mean diameter SMD or $D(3,2)$, i.e., the ratio of the third moment to the second one. This last mean diameter is the diameter of the sphere that has the same surface/volume ratio as the whole population, the most significant value as far as the surfactant adsorption is concerned.

$$D(4,3) = \frac{\sum_{i=1}^n f_i x_i^4}{\sum_{i=1}^n f_i x_i^3} \quad D(3,2) = \frac{\sum_{i=1}^n f_i x_i^3}{\sum_{i=1}^n f_i x_i^2} \quad [5]$$

where f_i is the frequency in number in class i , characterized by its central diameter x_i . The arithmetical mean m or first moment is calculated as:

$$m = M_1 = \sum_{i=1}^n f_i x_i \quad [6]$$

the degree of polydispersity is given by the standard deviation, symbolized by σ , which is the square root of the second moment around the first moment value.

$$\sigma = \sqrt{\sum_{i=1}^n f_i (x_i - m)^2} = \sqrt{M_2 - M_1^2} \quad [7]$$

m and σ are the two parameters that appear in the theoretical expression of the normal distribution density:

$$f(x) = k \exp\left[-\frac{(x-m)^2}{2\sigma^2}\right] \quad [8]$$

where k is a numerical coefficient so that the integral below the frequency curve is the unity. If the distribution is log-normal x , m and σ are replaced by their natural logarithms.

Drop size distributions are often plotted as frequency vs. logarithm of diameter, to test the symmetry around the first arithmetic mean value or first moment m of an assumed log-normal distribution, which is a quite common case.

If the distribution is symmetrical (in the selected scale) the mode corresponds to the median, that is 50% of the cumulated drop volume or number whatever the distribution is. Another way to

estimate the asymmetry is to calculate the third moment of the distribution around the mean, which is zero for perfectly symmetrical distributions.

$$s_3 = \sum_{i=1}^n f_i (x_i - m)^3 \quad [9]$$

The distribution shape and its changes are handy information on the emulsion formation process or its evolution. For instance the presence of two modes indicates two separate stirring processes, and could be related to the mixing of two emulsions or to improper stirring. An asymmetrical distribution with a long tail on the higher drop size, particularly in logarithmical scale, is indicative of incomplete mixing. The increase of the frequency in the same region as time elapses is a precursor signal of future stability problems. The disappearance of the left part of the main peak (smaller drop) is indicative of a slow ripening process. It is recommended that all practitioners exercise extracting information from the drop size distribution.

Another way to handle this statistical data is to plot the accumulative or integral distribution on a Gaussian or Log-Gaussian graph, sometimes called probability plot. In such plots the normal or log-normal distributions become straight lines. It is thus very easy to test the goodness of the fit and to calculate the two parameters that define the distribution. The splitting into several straight line segments is also indicative of multimodal distributions that can be easily separated. It is worth noting that such a way to represent a normal or log-normal distribution by a straight line is readily amenable to very simple and transparent regression analysis on any personal computer.

C. Stability

Although emulsion stability is not a concept with a well agreed upon definition, it is always linked either to the persistence or to the decay of the dispersed system under certain circumstances. As a matter of fact it is a fundamental emulsion property and a lot of attention has been dedicated to its study (10-11).

1. Involved Phenomena

The first question to answer is stability against what? In fact, an emulsion can remain unchanged under certain circumstances while it will break readily under others. Of particular importance are the eventual changes in temperature that have a formulation effect as seen in the previous chapter. Other emulsion breaking processes could include physical effects like artificial gravity, Brownian motion or stirring. However, the most common case however is when an emulsion is kept in a container to rest at constant temperature under normal gravity conditions.

This is the one to be dealt with here and later to be considered as a reference based on which other cases could be discussed. This breaking process comprises several steps: (a) long-distance

approach between drops or between drop and flat interface, (b) interdrop film drainage; and, finally (c) coalescence (10-13).

Since the continuous and dispersed phase have generally different densities, there is a neat Archimedes pull on the dispersed phase drops that drives a separation process called *settling*. This separation tends to gather the drops in a region that becomes a high internal phase ratio emulsion, sometimes referred to as a *cream*.

The settling process is essentially similar in nature to Stokes falling sphere sedimentation problem, eventually modified according to Hadamard's work (14) to account for the fluid motion inside the drop. The Stokes calculation of limiting falling velocity is solved by equating the gravity force to the friction force, which is taken as proportional to velocity (creeping flow) and proportional to the radius of the sphere R. Thus the limiting velocity turns out to be:

$$v = \frac{R^3}{R} = \frac{R^2}{\dots} \quad [10]$$

where \dots is a constant ($2/9$ in the case of Stokes' law), \dots is the density difference, and \dots the continuous phase viscosity.

Since Stokes problem addresses the case of a single rigid sphere sedimentation in an infinite medium, the actual problem with plenty of falling spheres (with different diameters, thus different velocities) could be depicted only qualitatively by such a law. For instance, the simultaneous falling of many drops results in a countercurrent in the external phase that would reduce the actual falling velocity. The interaction of falling drops with one another is also a factor that would reduce the falling velocity. Even more serious objections rise from the possible retardation effect produced by tension gradients along the drop surface (15).

This means that the value of the constant is of course to be determined experimentally in each case, and that Stokes' law is only indicative, and may turn out to be wrong when the internal phase proportion is high. In any case Stokes' law indicates that the approach of the drops would be facilitated and accelerated whenever the drop size or density difference increases, while it would be slowed down by an increase in external phase viscosity.

In the macroemulsion range (1-100 μm) the settling may be rather quick unless the external phase is viscous or the density difference is very small. In the miniemulsion range (100-500 \AA) the settling is generally very slow because of the importance of the squared radius factor. Thus, it may be said that an extremely small drop size would slow down the first step of the breaking process, and as such would slow down the whole process. This statement is true in the event that the second step (drainage) is rather quick, i. e., when the surfactant does not provide the appropriate stabilization conditions, so that the first step controls the decay.

The maximum internal phase ratio that can be attained without deforming the drop spherical shape depends upon the drop size distribution. For monodispersed rigid spheres, the most dense tessellation is the hexagonal packing at about 74 % of internal phase. As an example, for randomly settled monodispersed spheres it could be 65 %. For very polydispersed emulsions it might be higher than 90 % (16).

The final arrangement of the drops in the cream depends upon the segregation process between drops. In effect, if the density difference is large, the R^2 factor results in a considerably increased force on the large drops that would settle more quickly and end up accumulating at the far end of the cream. The shape of the settling vessel is also important in the segregation process because the segregation could be large if the settling path is long and vice versa.

Of course, if the emulsion contains more than 60-70% of internal phase, particularly with small drops, the settling would not take place significantly. In any case the Brownian motion or other unusual effects may provide some driving force for the drop-drop interaction to be dealt with in the next paragraph (17-18).

When the drops are close together, whatever the driving force that makes them approach, the film that is located in between neighboring drops exhibits a complex drainage process that involves several different mechanisms, and this controls the second step of the emulsion decay. Some of them depend upon the drop volume like the Van der Waals attractive forces, or the Archimedes pull, while others depend on the interdrop film physical properties such as viscosity, or on the interfacial phenomena that occur whenever two interfaces approach at sub micrometer range. The first class of interfacial phenomena deals with static attractive or repulsive forces, like electrical, steric or entropic repulsions, while the second one has to do with dynamic processes like the steaming potential and interfacial viscosity effects, as well as the more classical hydrodynamic considerations (19-23).

In some cases the interdrop film becomes very thin, only a few micellar or molecular sizes across. It decreases not continuously but stepwise, layer by layer, and could end up in a surfactant bilayer with no solvent content (sometimes referred to as black film because of its color). Such extremely thin films could exhibit a high resistance to rupture as it occurs in so-called foam emulsions (23-24).

In most cases, there exists an electrical double layer near the interface, even in absence of charged surfactant, in which case the differential adsorption of OH^- and H_3O^+ ions results in a net charge per unit area. As a matter of fact nonionic surfactants often produce a negatively charged interface at neutral pH because the smaller OH^- is more abundant in the vicinity of interface than the hydrated proton. In any case it can be considered that the double layer is a very general feature at liquid interfaces. Of course the charge separation occurs in a very thin region near the interface, whereas the whole electrical balance per unit area is neutral. As indicated in figure 3, the region is

split into an adsorbed or fixed layer and the "diffuse" layer in which the ions are free to move with the fluid, hence its name "double layer". In the diffuse layer the ions are submitted to an attractive force that pulls them back toward the opposite charge interfacial layer, and the random molecular motion, i. e., their escaping tendency. Several models have been proposed which are discussed in classic textbooks on surface science (25-27) or specialized publications (28-29).

The overall result is typically an exponential distribution of ionic charges in the diffuse layer that result in an exponentially decreasing potential according to the so-called Debye approximation:

$$\phi = \phi_0 \exp(-x/\lambda_D) \tag{11}$$

where x is the distance from interface and λ_D a characteristic parameter known as Debye length. ϕ is the potential at distance x from interface while ϕ_0 is its value at interface.

Debye length is somehow a measurement of the diffuse layer thickness, which is directly linked to the distance at which electrical repulsion between two approaching interfaces begins. In effect the pressure (force per unit interfacial area) produced by two diffuse layers overlapping may be expressed as follows in the case of approaching flat surfaces separated by a distance x :

$$P = \frac{2\epsilon_0\epsilon_r\phi_0^2}{x^2 \cosh^2(x/\lambda_D)} \tag{12}$$

It is seen that the repulsion is a function of both λ_D and ϕ_0 . It may be shown that as ϕ_0 and λ_D increase the repulsion takes place at a larger distance, a favorable feature for emulsion stability.

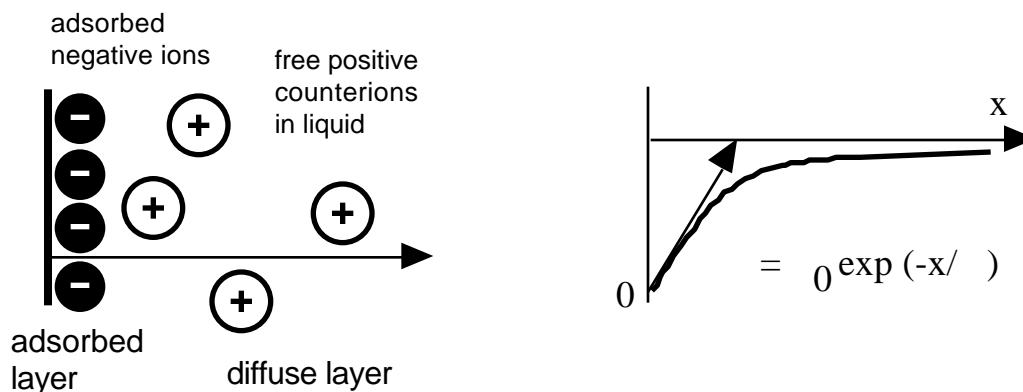


Figure 3: Electrical double layer and potential variation versus distance from interface

While λ_D is directly associated with the amount of adsorbed charges, e.g., ionic surfactant adsorption, λ_D depends on several factors as seen in the following equation.

$$\lambda_D = \sqrt{\frac{RT}{F C_i Z_i^2 \epsilon}} \quad [13]$$

where F is the Faraday constant, ϵ the permittivity of the medium, C_i the concentration of ion specie "i" in the bulk (out of the double layer) and Z_i its valence. This relationship indicates that an increase in electrolyte concentration, particularly with polyvalent species, would decrease the double layer thickness and thus the distance at which the repulsion is effective. Since attractive van der Waals forces are generally dominating at short distance, a repulsion effective double layer should be thick, so to speak, since this could mean 100 Å only. This antagonism of electrical repulsive forces and van der Waals attractive forces was the subject matter of the DLVO theory [name given after the people who proposed it simultaneously in Russia (Derjaguin and Landeau), and Netherlands (Verwey and Overbeek)] to explain lyophobic colloid stability in presence of electrolyte (30-32). This theory was a landmark in colloid chemistry history as the first successful attempt to explain complex experimentally known phenomena.

Today it contributes as a model for emulsion stability on a qualitative basis, since the drop size is much bigger than a colloidal particle, so that DLVO interaction calculations do not apply straightforwardly. Moreover it is now recognized that the repulsion between approaching drops may come from other (non-DLVO) interactions such as the steric repulsion between adsorbed molecules, which is the most common case with nonionic surfactant and polymer emulsifiers both in water and in oil (33-34). There is first an enthalpic contribution that has been referred to as osmotic repulsion as well, because it has to do with the departure of the chemical potential of the solvent in the region where adsorbed surfactant layers overlap (35). On the other hand, there exists another repulsion mechanism, often called entropic, that is related to the molecular organization or degree of freedom with respect to interactions of surfactant or polymer molecules with the solvent that change as the two interfaces get closer (36). Figure 4 illustrates the different cases of repulsion: electrical repulsion in presence of ionic surfactants and steric repulsions with nonionic surfactants, such as the polyethoxylated ones. The third type, i. e., entropic repulsion, for instance occurs when polymeric amphiphilic molecules are forced to rearrange and sometimes to lose solvation as they are compressed. As in DLVO theory, the overall balance of repulsive and attractive forces may result in different cases, since their variations are not necessarily at the same scale nor manner. For instance molecular attractive forces act at short range (x^{-6}), while electrical ones are rather long range forces (x^{-2}).

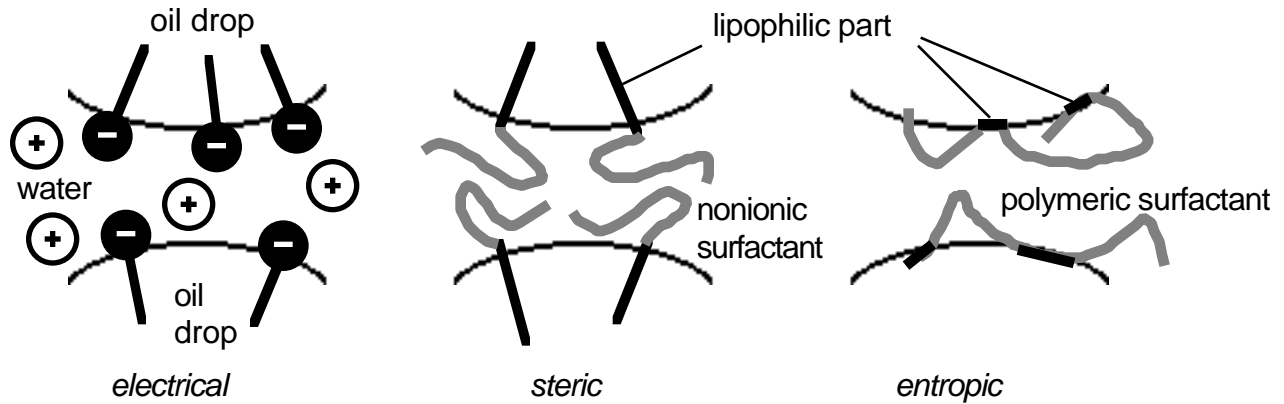


Figure 4: Three cases of interdrop repulsion

Steric and entropic forces do not produce any effect until some kind of contact takes place between adsorbed antagonist layers, at which point they can increase slowly or rapidly depending upon the compressibility or elasticity of the adsorbed layer. In many cases several effects can contribute.

There are essentially three cases as in DLVO theory, that are characterized by the shape of the repulsive-attractive potential vs. distance (see Figure 5). In the first case (left) the attractive forces dominate at all distance and thus the two approaching interfaces will get into contact sooner or later depending upon kinetic phenomena, as seen later on. The minimum of the curve (maximum attractive potential) corresponds to the notion of contact and occurs at an essentially zero distance (exaggerated in the figure). A further reduction in distance would be opposed by the compressibility of matter, and would result in a strong repulsion.

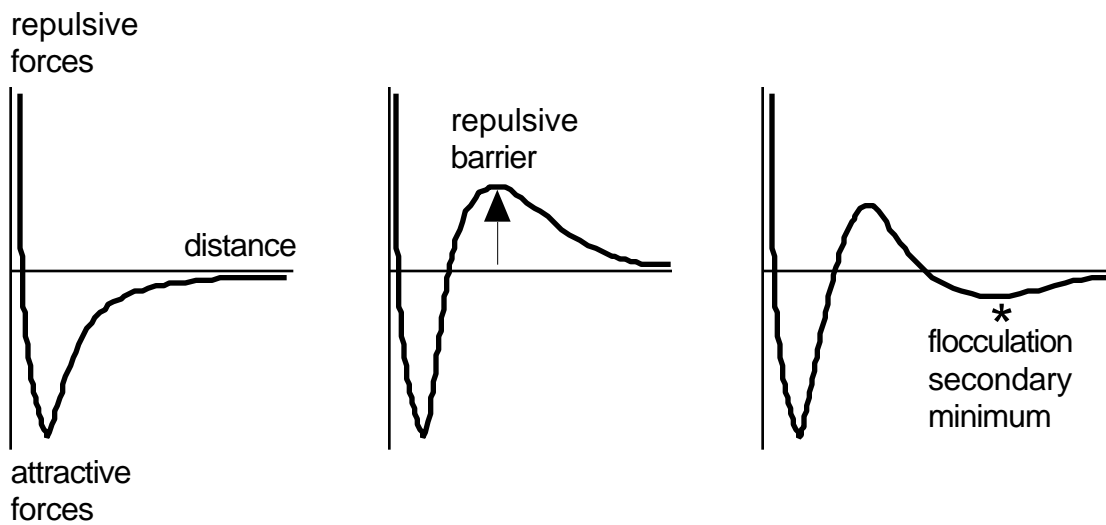


Figure 5: Three cases of variation of the interdrop forces versus interdrop distance according to the extension of the DLVO theory

At the maximum attraction distance solid coagulation and liquid drop coalescence would take place at once. The second case (center) is typical of a long range repulsion and a short range attraction as in ionic surfactant systems with low electrolyte content. As the distance between approaching interfaces decreases, the electrical repulsion dominates and reaches a maximum value. If this "barrier" is high enough, no drop would possess the sufficient kinetic energy to surpass it, and the repulsion would end up dominating, with a resulting stable emulsion. If the barrier is not high enough, a fraction of the approaching drops, those with enough kinetic energy, would reach the distance where the forces become attractive and would end up getting into contact and coalescing.

The third and most complex case exhibits the so-called secondary minimum. As interdrop distance decreases the force is first attractive, then it becomes repulsive, then attractive again. The long range attractive forces are weak forces so that the secondary minimum, which is located at a "large" distance is not very deep. Hence, a small amount of kinetic energy, like mechanical mixing, can offset it to redisperse the flocculated drops. It is worth noting that the distance at which the secondary minimum occurs is too long for the drops to coalesce. They are just linked by some weak attractive force and can be separated again, so that this is not to be considered as an instability phenomenon but rather as a reversible metastable association. This phenomenon often occurs when the repulsion forces of the second case are weakened, for instance, by adding electrolytes. Too much weakening could, however, lower the repulsive barrier so that the primary deep minimum is attained. There the distance is so short that coalescence will take place, and the energy hole is so large that redispersion would require an energy input similar to the one that allowed to make the emulsion in the first place.

Interdrop flocculation is not an uncommon phenomenon in high internal phase or creamed emulsion, and it generally results in a temporary increase in viscosity, yet this effect may be usually be reversed by applying a low-energy shear.

The previous discussion dealt with forces and potentials, i. e., equilibrium concepts, so that it indicated the possibility of occurrence of some events, not the velocity at which they could happen. These potential considerations may be brought into a kinetic model similar to a bimolecular reaction rate, in which the probability of coalescence is taken as a function of the repulsive potential. This leads to a second order kinetic model first proposed by Smoluchovski in 1916. It is useful to describe an emulsion ripening process in which the reciprocal of the number of drops in a given system increases linearly as time elapses. This model has been improved upon to calculate the coalescence dynamics of non deformable drops (37-38) as well as deformable drops associated to a thin film hydrodynamic drainage (39-40).

It is worth mentioning that a special issue of the *Journal of Dispersion Science and Technology* (41) has been recently dedicated to the research work of Bulgarian investigators on thin films and related topics, as a tribute to their outstanding contribution to the field.

There are also other dynamic phenomena to be somehow accounted for (20, 42). For instance, the approaching of two droplets occurs simultaneously with the drainage of the interdrop liquid, in which fluid dynamic phenomena may bring in several other kinetic features. For example, in presence of an ionic surfactant such as sodium dodecylsulfate, the amphiphilic dodecyl anion would adsorb at interface while the sodium counterions would stay in the aqueous bulk phase. In such a case the negative charges are somehow "attached" to the interface, while the positive ones are linked to the liquid. When the two drops get closer, the liquid film withdrawal strips away electrical charges from the electrical double layer, which creates a charge separation. This results in the streaming potential effect, which tends to return the charges to their initial position. As a consequence, the film drainage is slowed down and everything happens as if the film liquid were much more viscous than it actually is. This is why this phenomenon is also referred to as electroviscosity.

The presence of adsorbed molecules that bear interactions with the film liquid phase, e. g. by solvation, may result in the interfacial viscosity effect, in which the motion of the liquid is transmitted to the adsorbed molecules that cannot move freely because of lateral interactions with other adsorbed molecules (43-44). This may happen particularly with macromolecular species, often known as colloid protectors, that also exhibit a viscosity enhancing effect in the bulk phase. All these effects can reduce the interdrop film drainage rate and thus determine the long term persistence of the emulsion.

It is considered that unless the final instantaneous step, i. e., drop coalescence has occurred, the emulsion is not broken since it can be redispersed with an amount of energy which is often much smaller than the one required to make the emulsion in the first place.

These were the typical situations dealt with whenever an emulsion was left to decay in the gravity field at constant temperature. If this is not the case, the actual occurrence might depend quite a lot upon the circumstances of the emulsion exposure to decay, like changes in formulation, temperature, or WOR (drying), as well as stirring. Only trends are known as far as these effects are concerned, and it can be said that even the commonplace emulsion decay at rest under normal gravity is too complex to be fully interpreted in a quantitative way.

2. How to Measure Stability

It is said that an emulsion is stable when it does not change its aspect in three years or so, and that it is unstable if it has completely separated after a few minutes. Anything in between these extremes requires a quantitative measurement of the emulsion evolution with time.

The unique absolute measurement would be to count the number of drops in a given container, an information that cannot be collected without altering the system, so that only a single measurement may be done, which is not very sagacious anyway. The second choice would be to

analyze a sample of the emulsion from time to time to determine whether the drop size average and/or distribution is changing. This could be done with some accuracy, but a lot of inaccuracy may come from the sampling process. In effect, if the emulsion is left to rest in the gravity field, the settling would result in a segregation by size according to a vertical distance. Thus, the sample drop size is likely to depend upon the location where the sample is withdrawn. The answer to this problem is to not take the sample at the same location, since such a tactic could backfire. For instance, if the sampling is taken exactly at the middle of a test tube that contains an emulsion containing small and big oil drops in water, the first change to be observed could be an increase drop size because of the transit of the big drops that were initially in the lower part of the test tube, then a return to the initial average size, then finally a decrease in drop size after all big drops have settled into the upper part. It is obvious that such a segregation could completely hide the way the drop size changes because of coalescence.

The experimenter could be rid of this obstacle by completely remixing the whole system before taking a sample. However, such a procedure would destroy the rest state of the emulsion by interrupting any segregation or flocculation process. The final solution of this problem, is to prepare several small samples in separated vials to be kept exactly in the same conditions until each of them is opened and fully mixed before carrying out a drop size measurement. This may not be satisfactory for some unconventional studies that would require large emulsion amounts to be kept or turned upside down in a jar or submitted to heating-cooling cycles as in real life occurrence.

In many instances the concept of emulsion stability is linked with a visual change in appearance or tactility, i.e., because some portion of one or the two phases separates from the emulsion, or because some other crucial property such as viscosity is significantly altered. If the emulsion is not too stable this may be a nice way to follow up the decay. If it takes too long a time to get visible measurable changes, then some time acceleration tactics would be advised.

Figure 6 indicates the typical variation of separated oil or water volume from the emulsion as times elapses. The separated volume V_c could come from the internal phase drops that have coalesced or could be the external phase which has been cleared from settling drops. V_∞ is the same phase volume value at infinite time, i. e., after complete settling, so that the V_c/V_∞ ratio varies from zero to unity.

The second occurrence (external phase clearing) is not necessarily a measurement of instability since the gathering of drops in a cream without coalescence could be reversed by an appropriate slow mixing.

This clearing and creaming is common in low-internal-phase-ratio emulsions, in which there is a large density difference and large drops. If the experimenter is looking for a solid basis to study formulation effects for instance, a unit WOR is advised as well as the making of rather small

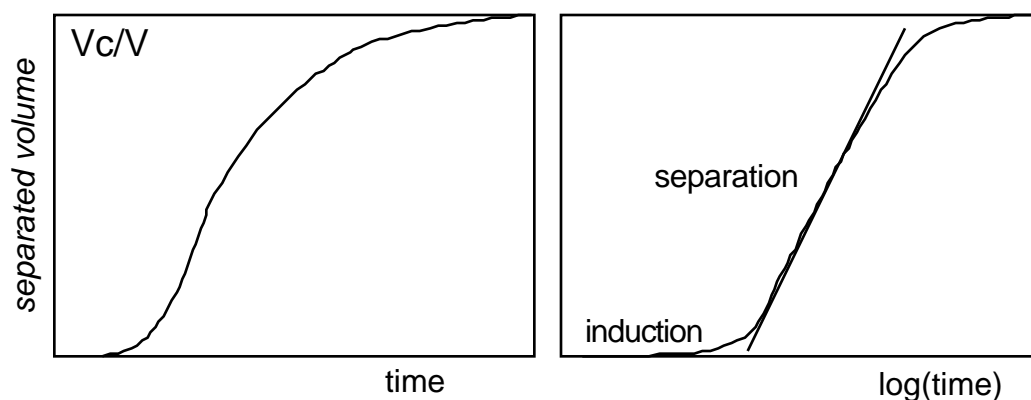


Figure 6: Variation of the separated phase volume vs. time.

drops to eliminate this eventuality. If this is not possible, the monitored phase separation should refer to the internal phase only.

Coming back to Figure 6, it is seen that the apparent decay occurs in three periods. First, there is a period of time in which no separation takes place. This induction period may be related to the drop approach and film drainage, with no coalescence occurrence, so that no drop big enough to settle quickly is formed.

In the second period the separated volume increases steadily with time according to a S-shaped curve as indicated in Fig 6. This is when most of the coalescence takes place at a steady rate.

The third period is some kind of asymptotic behavior during which the last and smaller droplets complete their separation. This could trail quite a long time since the scarcity of droplets shrinks the probability of encounter and coalescence. Often, the central part of the separation curve is found to be linear vs. a logarithmic time scale, and the use of such a scale is advised to compare emulsified systems with very different stability.

3. Acceleration Tactics to Measure Stability

Some emulsions are sometimes so stable that they require an extremely long time to start separating, which is quite inconvenient when experimental time is money. It is thus worthwhile to try to artificially accelerate the emulsion breakup in order to compare formulation effects at a shorter time scale.

The first thing that comes to mind is to use a centrifuge to speed up both early sedimentation and ensuing creaming, and to augment the force that pushes the drops against one another and thus helps in the film drainage. This will in general accelerate the separation process, but it may also convey false or misleading information. In effect, some emulsions would never coalesce in normal gravity, while they would do it under artificial gravity, because of different

relative strengths between gravity and repulsive forces. In other cases, the creamed emulsion often will not coalesce either with natural or artificial gravity because the gravity pull has very little or no effect upon the surfactant role in slowing down the interdrop film drainage that commands the second and often crucial step in the separation process. The separation under centrifugation is thus a useful technique but not a necessarily successful even for comparison purpose.

Another method is to make an emulsion with a larger drop size so that the settling process is accelerated. A larger drop size also means a smaller surface to volume ratio, that is a lower repulsive effect (that depends upon the adsorbed surfactant at interface) vs. a higher attractive force (that depends upon the drop volume). This will lead to a reduction in separation time, although probably no more than one order of magnitude, which might be too little in many instances. This method influences the separation second step and is thus more reliable than centrifugation to predict trends.

A clever method is to reduce the stabilizing agent concentration at interface so that all the stabilizing phenomena taking place in the second step (that dominates the decay of stable emulsions) would be weakened. A reduction in surfactant concentration in the whole system is not appropriate to produce such a reduction in surfactant adsorption. In effect, it is known that the surfactant adsorption starts occurring at very low concentration, much lower than its critical micellar concentration CMC, while the surfactant concentration in stable emulsions is often much higher in order to insure a quick drop coverage during emulsification. Accordingly, a reduction in surfactant concentration is likely to first produce alterations in the emulsification process, and thus the emulsion would be quite different from the one that must be studied.

It is preferred to reduce the interfacial surfactant concentration without reducing the surfactant concentration in the bulk phase. This may be done by introducing a co-surfactant that would compete with the surfactant for interfacial occupancy, but would not provide the stability features the surfactant molecules do. The most likely candidates for such a purpose are short chain alcohols in the three- to five-carbon range. In order to occupy a larger interfacial area, the alcohol should not be too hydrophilic or lipophilic. The best intermediate choice seems to be in-between n-propanol and n-butanol, the first one being rather hydrophilic and the second more lipophilic. A mixture of these two n-alcohols, as well as secondary butanol, and even tertiary pentanol, would do the job fairly well at a 2-3 wt.% concentration level in the system. It is worth noting that these alcohols will exhibit a neutral hydrophilic-lipophilic tendency that will not significantly affect the formulation at interface. In the previous chapter, sec-butanol was attributed an $f(A)$ value of -0.16 at concentration above 3%, which is equivalent to a 15% increase in salinity or a reduction in one ACN unit in oil nature - a change which is smaller than the typical increment in a formulation scan, and thus is within formulation accuracy limits, unless a special fine tuning is sought.

Methanol and ethanol are mostly water soluble, but if they are added at the 10% level in water they will produce a significant lowering in surfactant interfacial effect by reducing the polarity

difference between oil and water. Higher alcohols (n-butanol to n-hexanol) would dilute the surfactant at interface, but would shift the formulation toward more lipophilicity, and thus alter the physicochemical formulation of the system. Even more lipophilic alcohols (above hexanol) are found to be mostly miscible with oil with little adsorption at interface, so that their diluting capability vanishes. However, they are known to produce an interesting effect in the oil side of the interface either as a lipophilic linker or as a polar oil. If some alcohol is already present in the emulsion, the addition of 1 or 2% of sec-butanol might be effective or not depending on the effect of the alcohol added in the first place.

The recommended addition of up to 3% sec-butanol could be realized before or after emulsification, but preferably before as an admixture to the aqueous phase, since it guarantees the best homogeneization. In many cases the addition of sec-butanol is found to considerably reduce (100-fold or 1000-fold) the time scale of the emulsion decay without altering its characteristics. However, the actual "accelerating" factor cannot be forecast by any means.

4. Quantifying Stability Measurements

There are two ways to quantify the notion of stability from the separated volume data as indicated in Figure 7, where the coalesced volume V_c (referred to as a fraction of its maximum value V) is plotted vs. time (as logarithmical scale) for two emulsions labeled A and B.

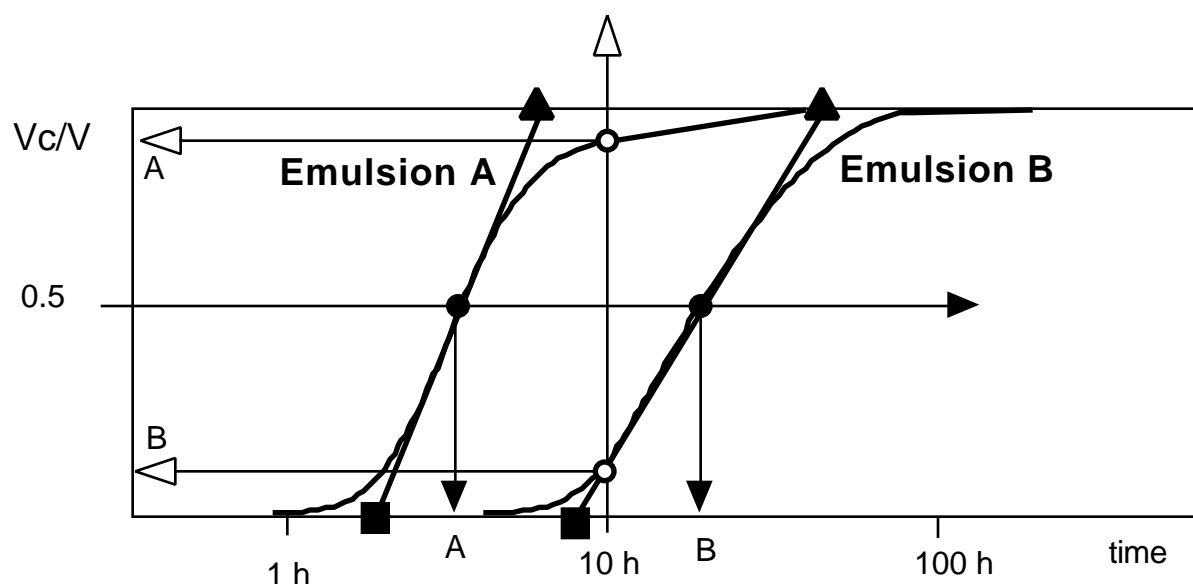


Figure 7: Comparison of the stability of two emulsions (A and B) according to the criterion defined in figure 6.

From the first glance it is obvious that the same trends apply to both emulsions, but earlier in the case of emulsion A which may be qualified as less stable. The way to quantify this concept is to intercept the two curves by a single line. For instance the (vertical) white head arrow located at a fixed time (here 10 h) intercepts both curves at a point (white dot) whose ordinate indicates the coalesced volume after ten hour. It is larger for emulsion A, which is thus less stable. In the present case there is quite a difference in coalescence fraction V_c/V between the two emulsions. However this is not the general case, since the emulsion coalesced volume fraction does not vary but over a sometimes narrow period of time. For instance, if the interception is made at 100 h instead of 10 h, then both emulsions are completely coalesced, while after 1 h none of them has started to coalesce. Thus at 1 h and 100 h the diagnostic is the same for both criteria, in discrepancy with the actual difference.

This is why the preferred method is to intercept the curve with a horizontal line, e. g., the (horizontal) black head arrow located at $V_c/V = 0.5$. The corresponding (black circle) intercepts indicate the times required for both emulsions to exhibit one-half settling. It is worth noting that since the curves are very similar in shape (with a logarithmic time scale), the result is essentially the same whatever the position of the intercept line. In some cases the incipient (respectively final) separation is the critical criterion and a 10% (respectively 90%) separation may be taken instead. Since in most cases the lower and upper regions of the curve do not exhibit abundant experimental points, an extrapolation of the central linear trend to zero and total separation (squares and triangles) could lead to a good comparison criterion.

D. Emulsion Viscosity

1. What is Really the Emulsion Viscosity

At a sufficient large scale, say 100 or 1000 times the drop size, the emulsion is generally considered to be an homogeneous substance, with constant rheological properties, provided that no change in emulsion characteristics takes place during the motion. This assumption means that there is no segregation phenomena, either by gravity or centrifugal acceleration, that would rule out the homogeneity assumption, or increase in drop size (e. g., by coalescence) due to the development of instability, or decrease in drop size (e. g., by breakup) due to shearing effects. In other words, emulsion rheology deals with stable nonsettling emulsions submitted to mechanical stresses that do not produce any characteristic change.

It is worth noting that these conditions might be too restrictive for many practical applications, so that only an approximation to real world effects could be expected. The situation is made even more complicated by the fact that in presence of surfactant, interfacial effects are likely to produce a pseudodiscontinuity at the macroscopic scale, e. g., a slipping velocity at wall or a tension

gradient at interface. If the wall is not completely wetted by the external phase, as it could happen with rough surfaces, then boundary conditions often become untractable. Moreover, emulsions are often non-Newtonian time-variable fluids with complex rheological behavior, so that it is a clever practical stance to keep expectation at the level of an apparent viscosity concept that would indicate the resistance to flow in some specific conditions, and would allow comparisons.

This is the posture taken in this chapter since rheological intricacies are discussed in details in another chapter of this book. The next section deals with the effects of physical variables on viscosity (1, 46). Later in this chapter, the crossed effects between physical properties, formulation, composition and stirring will be analyzed.

2. Influence of Physical Variables on Emulsion Viscosity

The dependency of emulsion viscosity upon different physical variables has been known for quite a while. It is generally written as proportional to the external phase viscosity:

$$\eta_{em} = \eta_{ext} f(\text{other variables}) \quad [14]$$

where the subscript "em" and "ext" refer respectively to the emulsion and to its external phase, and where $f()$ stands for the other effects contribution, i. e., those that do not depend upon the external phase. Obviously $f()$ is required to tend to unity as the internal phase content (habitually as volume fraction ϕ_{int}) tends to zero. This relationship is assumed to be valid in all cases, even with high-internal-phase-ratio emulsions, and other real world situations for which it cannot be experimentally verified. If the external phase exhibits a special behavior such as non-Newtonian or viscoelastic, this behavior is directly transferred to the emulsion through the external phase viscosity term.

The ratio of the emulsion viscosity to the external phase viscosity is often called relative velocity, and it is noted r instead of $f(-)$.

$$r = \frac{\eta_{em}}{\eta_{ext}} = f(-) \quad 1 \quad \text{as} \quad \phi_{int} \rightarrow 0. \quad [15]$$

The second and often most important influence is due to the internal phase presence. If drops are scarce, they are too far away to interact between them and the only interaction beyond the homogeneous fluid case, is that of each drop with its surrounding fluid. The increase in viscosity due to this interaction in the case of rigid spherical drops was calculated by Albert Einstein, who has been generally known for other scientific achievements, as:

$$r = 1 + 2.5 \phi_{int} \quad [16]$$

Equation [16] is essentially valid up to $\phi_{int} = 0.02$, and is useful only as to indicate the trend at origin. When the number of drops increases, the drop-drop interactions become predominant and the resulting frictional effects drive the viscosity increase.

If all the drops are rigid spheres with identical size, the densest tridimensional arrangement is the so-called compact hexagonal packing that fills 74% of the space. Thus, in the most favorable case, the maximum value for ϕ_{int} is 0.74, at which viscosity is infinite. In practice such an arrangement cannot be attained and essentially infinite viscosity is reached with monodispersed system at 65-70% internal phase content. However, emulsions are not generally monodispersed systems, but contain a distribution of drop sizes, so that small drops can enter the void space between larger drops. Moreover, liquid drops are not rigid spheres either and some deformation is likely to take place, up to the superlative case of polyhedral foam like structures. As a consequence, it may be said that there is essentially no limit to ϕ_{int} . Nevertheless, it is worth remarking that emulsions with more than 60-65% internal phase generally behave as complex fluids for which the concept of viscosity is no longer sufficient to describe the flow behavior.

Figure 8 indicates a typical variation of viscosity with internal phase content. It is seen that the increase in viscosity with the internal phase proportion starts slowly then turns faster and faster, until an almost vertical variation is registered near the emulsion inversion ϕ_{inv} value, here at about 82 % of internal phase.

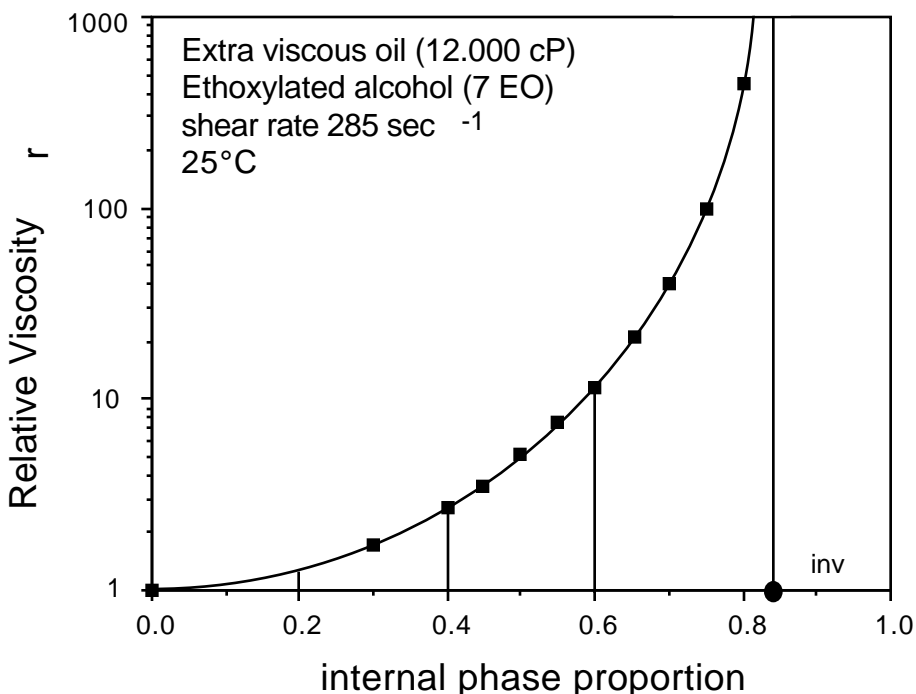


Figure 8: Typical variation of an O/W emulsion viscosity versus the amount of internal phase (49)

In most cases, the concavity points up, even when the viscosity scale is logarithmic. Many studies have reported empirical relationships to describe this behavior, but none are valid in the general case, because many other effects, particularly the non-Newtonian behavior, that are dissimulated in the η_r relative viscosity, are to be considered as well (47-48).

Hence, such a plot should be prepared for the particular application and emulsifying device to be dealt with. As far as some advice could be helpful, it may be said that above 60-70% internal phase, most emulsions become pseudoplastic fluids and their viscosity depends on applied shear rate, often according to a power law model. Above 85-90% internal phase, the emulsion does no longer behave like a simple fluid and a viscoelastic description is often useful.

In many cases Pal's empirical equation (48) has been found to provide a fair approximation up to 70-80% internal phase, maybe because it contains experimental data η_{100} as the η_{int} value at which $\eta_r = 100$. This experimental value has to be attained in the same conditions, particularly stirring characteristics, which may be why it significantly embodies the global effects of all remaining variables beyond η_{ext} and η_{int} .

$$\eta_r = \left[1 + \frac{\eta_{int}/100}{1.187 - \eta_{int}/100} \right]^{2.49} \quad [17]$$

As a matter of fact, the internal phase content is the most important variable as far as the viscosity of high internal phase ratio emulsions is concerned, and provided that the formulation insures a proper stability.

The third kind of variable to be dealt with is the drop size average value and distribution. Since the overall emulsion surface area depends upon the square of the drop size, while the internal phase volume depends upon the cube of the drop size, the surface-to-volume ratio changes as the inverse of the size. In other words, small-drop emulsions exhibit a higher surface area per unit volume than big-drop emulsions. Since the interdrop friction effect is related to the surface area of the drops, an increase in viscosity is expected to be associated to a decrease in drop size.

Most experimental studies on monodispersed systems were carried out on solid dispersions rather than emulsions, since it is quite tedious to get a monodispersed emulsion. Experimental evidence from narrowly dispersed emulsions shows that the viscosity increases as the drop size (average) decreases, often according to an inverse power law such as:

$$\log \frac{\eta}{\eta_0} = -B \log \frac{d}{d_0} \quad [18]$$

where the "0" subscript indicates a reference state. In some cases of not-too-severe stirring, B is found to be near unity, although it is less if an energetic stirring is provided. Also in this case, an

experimental approach is advised since many other variables are interfering, as well as the very selection of the formula to compute the drop size average.

The drop size distribution is found to play an important role as well. In effect, a mono dispersed system contains at least a 26% void volume, that may be filled with much smaller droplets, and which could occupy up to 74% of this volume, thus leaving 7% (= 26% x 26%) void and so on. This means that a polydispersed emulsion is generally less viscous than a monodispersed one with the same drop size average, no matter the way the average is calculated. There is no empirical relationship to render this effect, but it may be said that it is significant when the ratio between the extreme diameters at 90 and 10% of the distribution in volume, respectively $D(v,0.9)$ and $D(v,0.1)$, exceeds 5.

The most spectacular viscosity reduction effect is with bimodal emulsions, which exhibit a distribution curve with two maxima, in most cases as the result of mixing two emulsions. These biemulsions are frequently found to be less viscous than their base emulsions whenever the difference in average sizes or mode separation is large enough. Most of the bimodal dispersion studies have been carried out on solid suspensions instead of emulsions (50-52); however, the results seems to be directly applicable to emulsions. Figure 9 indicates such a case attained by mixing emulsions with identical internal phase ratio but different sizes, with a mode separation measured as the corresponding diameter ratio is 3 (53).

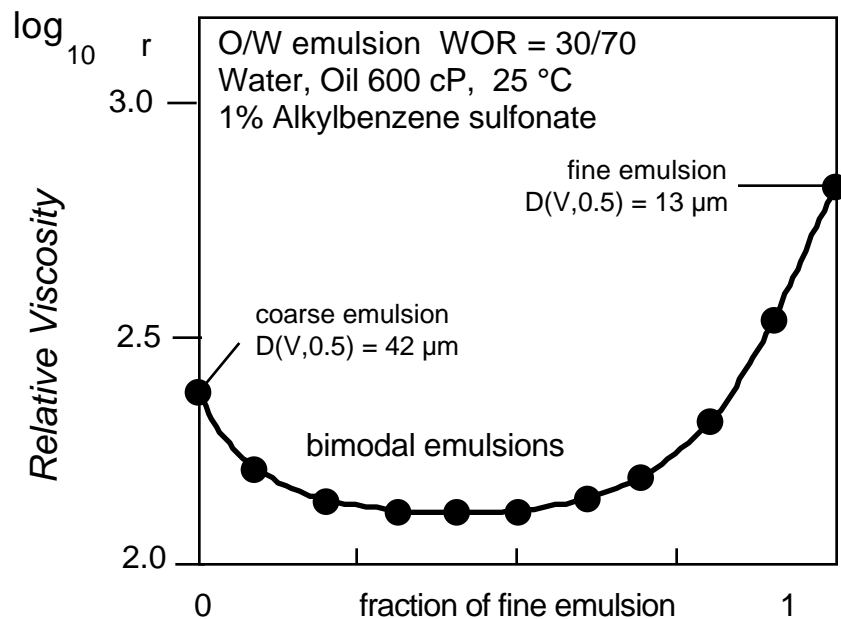


Figure 9: Variation of the viscosity of biemulsions made with two emulsions with the same water/oil ratio but different drop size, versus the proportion of fine emulsion in the mixture (54).

It is seen that a considerable viscosity reduction is attained by mixing a fine emulsion with a coarse one, over a wide range of composition (54). However, the effect depends upon the relative polydispersity of each emulsion and it is most spectacular with a narrowly dispersed coarse emulsion and a polydispersed fine emulsion with no overlapping. This technique has been proposed for reducing viscosity in crude oil emulsified transport (55), or coal slurry flow (56), but it may also be readily applied for producing less viscous cosmetic milks or lotions and pharmaceutical emulsions with high internal phase ratio.

Some literature reports confirm the intuitive feeling that the internal phase viscosity should have an effect upon the emulsion viscosity. This is quite misleading for the following reasons. First of all, most emulsion droplets are so small that capillarity makes them perfectly spherical. Second, the shear imposed to get an emulsion flowing is generally much less severe than the one used to make the emulsion in the first place. Note that if this is not true, one of the basic assumption stated in the first paragraph of this section is not complied with. With a low shear stress level, the momentum is not transferred inside the drops that may be regarded as rigid spheres. If there is no motion in the internal phase, there is no way to relate any effect to the viscosity of this phase since the viscosity is a meaningless concept at rest.

Therefore, the internal phase viscosity must not alter the emulsion viscosity. The often reported trend that a higher internal phase viscosity is associated with a reduction in emulsion viscosity is indirectly due to a change in drop size. In effect, under identical stirring conditions, a viscous internal phase might not break up as easily as a less viscous one, thus resulting in larger drops and lower emulsion viscosity. These phenomena are linked with the rupture and coalescence mechanisms during emulsification. They have been discussed in detail in the literature, although not often in presence of a surfactant (57-65).

Other effects are likely to influence emulsion viscosity, particularly high-internal-phase-ratio emulsions in which the drops are separated by thin films. Both dynamic phenomena such as streaming potential or interfacial viscosity retardation could take place during the drainage of these films. Electrical and steric repulsion, as well as surface hydration are probably also important in these kinds of emulsions. These phenomena that are due to the presence of adsorbed surfactant onto approaching interfaces, have been studied in relation to stability problems but not for their effect on viscosity. It can be said however as a rule of thumb that any effect that would tend to reduce the flow of interdrop film would result in increased viscosity or, rather in impaired flowing ability.

On the other hand it has been discussed in the previous chapter that formulation can greatly influence interfacial tension, a crucial factor in the determination of the breakup-coalescence dynamic equilibrium and thus the drop size average and distribution. Consequently it is no wonder that - last but not least - the physicochemical formulation influences emulsion viscosity. The

approach to be presented here is based on experimental facts because theoretical considerations are not proficient enough to give a whole comprehensive picture.

For the sake of simplicity, the influence of formulation is to be presented on all emulsion properties simultaneously, which is the most logical way of analyzing the results since the properties are not independent, e.g., the drop size influences viscosity and stability.

II. INFLUENCE OF FORMULATION ON EMULSION PROPERTIES

Experimental studies that were carried out to analyze the influence of formulation upon the emulsion conductivity, stability, viscosity and drop size, indicate that there exists a general phenomenological pattern of variation for all tested systems.

The following results are quite general for systems containing roughly equal amounts of oil and water, e.g., from 30 to 70% of any of them, and a very few percentages of surfactant. This limitation on the water-to-oil ratio is stated to exclude high-internal-phase-ratio emulsions, for which the composition is found to have a strong influence, as will be discussed in the third section. The small amount of surfactant insures that the system's representative point falls inside the multiphase region of a ternary diagram. In order to avoid any special effect coming from the mixing protocol, a turbine blender is used to provide isotropic turbulent stirring.

The investigation technique is the unidimensional formulation scan as in the phase behavior studies discussed in the previous chapter. For the sake of simplicity, the scanned variable is often taken as the salinity for ionic surfactant systems, and as surfactant EON or temperature for nonionic systems, but it should be well understood that other formulation variables would produce exactly the same effects. In the reasoning, the formulation will be referred to as SAD, the deviation from optimum formulation, whatever the variable used to produce the scan.

A. Conductivity – Emulsion Type Change

Figure 10 indicates the change in conductivity along two formulation scans (66). For each formulation a test tube is left to equilibrate during several hours or days, and it is then emulsified according to a standard stirring protocol. The electrolytic conductivity is then measured. The left plot indicates the conductivity change along a salinity scan with an anionic surfactant system. At low salinity $SAD < 0$, and the surfactant dominant affinity toward the aqueous phase results in a curvature that favors the O/W type, as corroborated by the high conductivity value. As the aqueous phase salinity is increased, the conductivity increases, since the ϵ_{ext} proportionality term increases (see previous section on conductivity).

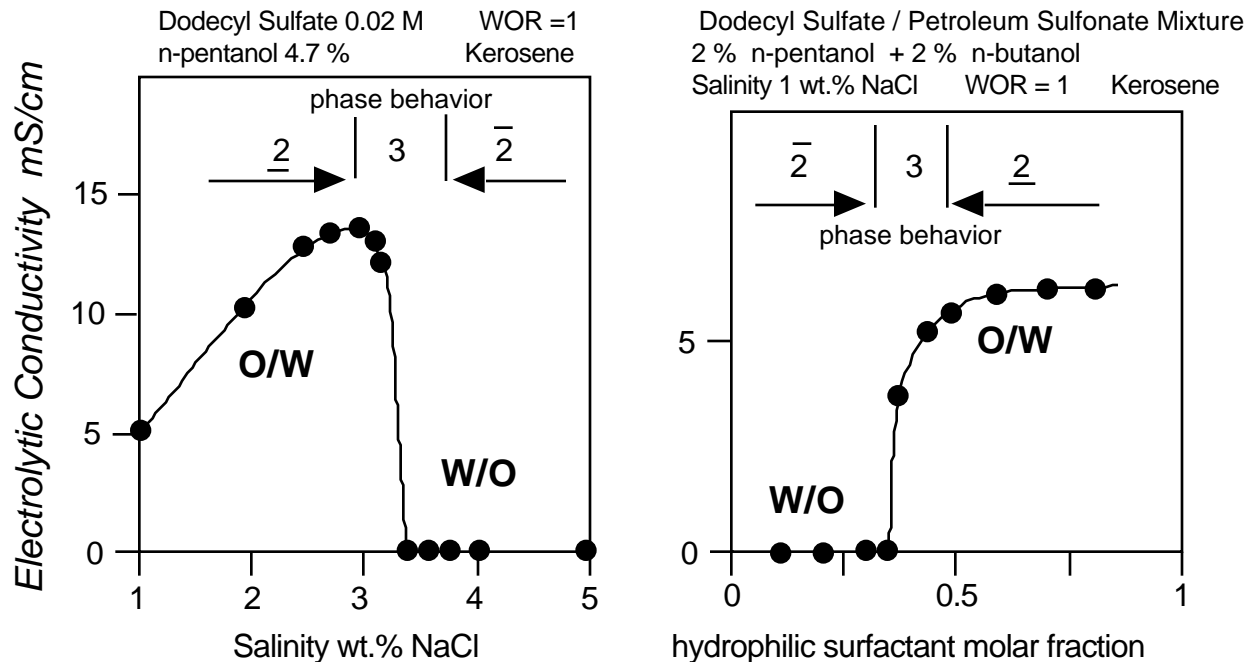


Figure 10: Variation of the emulsion conductivity along two formulation scans. Salinity scan (left) and surfactant hydrophilicity scan (right). After reference (66)

In the vicinity of optimum formulation ($SAD = 0$), the conductivity decreases rapidly as an indication that the emulsion is now of the opposite W/O type. The formulation at which the emulsion changes from one type to the other is thus near optimum formulation, inside the three-phase behavior zone.

The right plot indicates the variation of conductivity as a function of surfactant hydrophilicity, by mixing a low hydrophilicity petroleum sulfonate with sodium dodecylsulfate. As the mole fraction of hydrophilic dodecylsulfate increases, SAD decreases, as opposite to the previous scan. It is also seen that the conductivity increases near $SAD = 0$ in the three phase behavior region. This time the conductivity stays at a constant value for $SAD < 0$, since the salinity of the aqueous phase is unchanged during the scan.

Many experimental results show that when the formulation is scanned through optimum formulation, the emulsion conductivity changes from high to low (or vice versa depending upon the direction of the effect of the scanned variable).

This means that the emulsion type switches at optimum formulation, with O/W emulsion on the negative SAD side and W/O on the positive one, according to Bancroft's rule. Fine-tuning experimentation shows that the change from O/W to W/O or vice versa, takes place not at a precise point, but rather over a narrow range of formulation. As illustrated in figure 10 right plot, it is

sometimes possible to pinpoint some intermediate conductivity value in the three-phase behavior region, which is probably related to the existence of bicontinuity either in the emulsion or in its external phase which could be the microemulsion.

B. Emulsion Stability

In what follows, the emulsion stability is measured after the settling curve, as indicated in the previous section on stability. However, the results of this section are quite general and independent of the method used to estimate stability.

Figure 11 indicates the separated volume of internal phase (as V_c/V_c) vs. time (log scale) for several emulsified systems corresponding to the formulation scan already studied in Figure 10 (left). The formulation is indicated by the salinity of the aqueous phase, that changes from 1.8 to 7.6 (wt.% NaCl). Three phase behavior ranges from 2.8 to 3.8 % and optimum formulation is located at about 3.4 % salinity. Figure 11 indicates the relative amount of coalesced internal phase (V_c/V_c).

It is worth noting that in this kind of plot, all settling curves exhibit the same shape, a quite remarkable fact since the time scale extends over four orders of magnitude. This allows one to classify the emulsion stability according to the position of the curves in respect to one another.

As the salinity of the aqueous phase increases the settling curve moves from the extreme right (high time equivalent to high stability) to the left (low time equivalent to low stability), then moves back to the right (high stability again). The minimum stability is attained for a salinity (3.4 %) corresponding to the center of the three-phase range, i. e., at or very near optimum formulation.

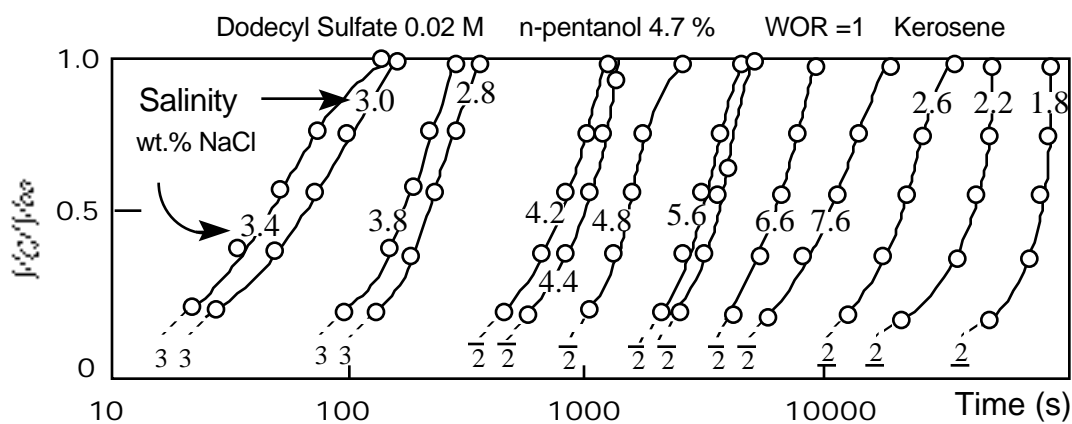


Figure 11: Relative separated volume of aqueous phase versus time for a series of emulsified systems along a salinity scan. (66)

A better diagnostic could be apprehended if the stability is taken as the time t_c required for a certain settling to take place, e. g., $V_c/V_c = 1/3, 1/2$ or $2/3$ as plotted versus formulation in Figure 12. On such a plot the minimum stability is even more evident, and it is seen to be essentially independent from the selected V_c/V_c value. The occurrence of a stability minimum at optimum formulation is a very general feature that has been found in many different systems with no exception known (42, 66-72). Various explanations have been advanced by different researchers to interpret this occurrence, such as the trapping of the surfactant in the microemulsion phase (73), the formation of liquid crystalline bridges (74-75), or the instability of a hole in the interdrop film (76). Whatever the right justification, the result is quite consistent with the wedge theory prediction that at optimum formulation the natural interface curvature is zero, and thus the surfactant cannot stabilize any type of emulsion that would imply the existence of a natural non zero curvature.

Note that the variation of the emulsion stability is extremely rapid near optimum formulation, while it is much less at some "distance" from it. Also note that in figure 12 case the variation of emulsion stability is not exactly symmetrical with respect to optimum formulation. In fact it could be more or less symmetrical, depending on the case, and there is no general rule on that since there are other reasons for O/W and W/O emulsions to exhibit different decay rates. In particular the formulation variable selected to carry out the scan could affect the two types of emulsion in very different ways.

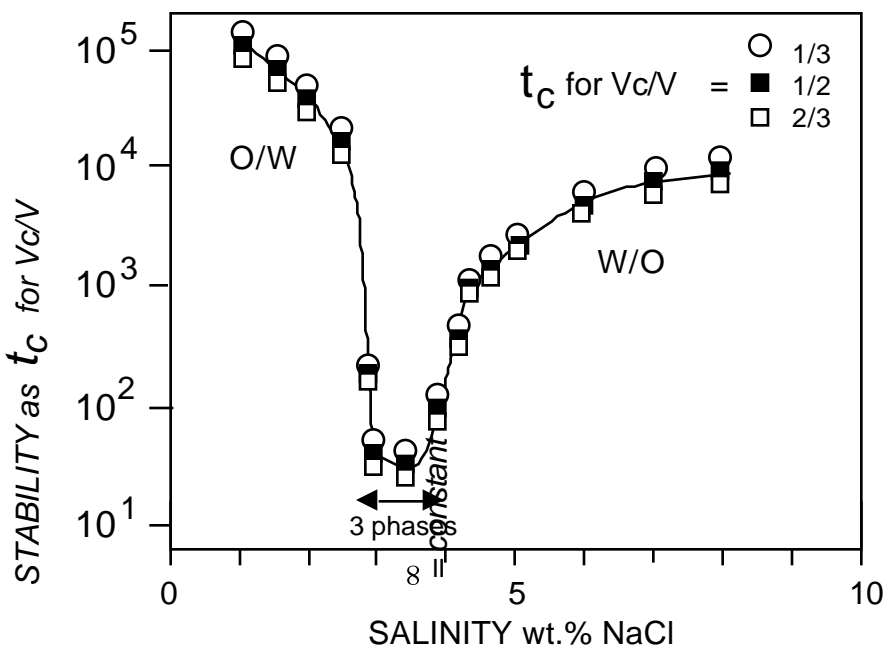


Figure 12: Variation of the stability of the emulsified systems, as the time required to separate a given relative volume of aqueous phase, for a salinity scan (66). Same systems as figure 11.

C. Viscosity

As for the study of conductivity, a series of emulsions are prepared along a formulation scan, and their viscosity is measured by any standard method. Figure 13 (left) indicates the variation of the emulsion viscosity in the case of a near unity water-to-oil ratio, and oil and aqueous phases with similar viscosities. In such a case the variation is roughly symmetrical with respect to optimum formulation (77). The viscosity minimum located at optimum formulation is easy to detect but difficult to measure since the corresponding emulsions are extremely unstable (see previous section). It is believed that this low viscosity is linked with the occurrence of extremely low interfacial tension, which allows the drops to elongate very easily along the streamlines.

Figure 13 right indicates a similar scan but this time with a paraffinic oil, which is much more viscous than water. As expected from the proportionality relationship between the emulsion viscosity and its external phase viscosity, W/O emulsions are much more viscous than their O/W counterparts. Nevertheless, a slight minimum is found at optimum formulation in spite of a strongly asymmetric shape.

The viscosity minimum is found in all cases in the vicinity of optimum formulation, and it is generally more discernible with nonviscous fluids and extremely low tension systems (77-79).

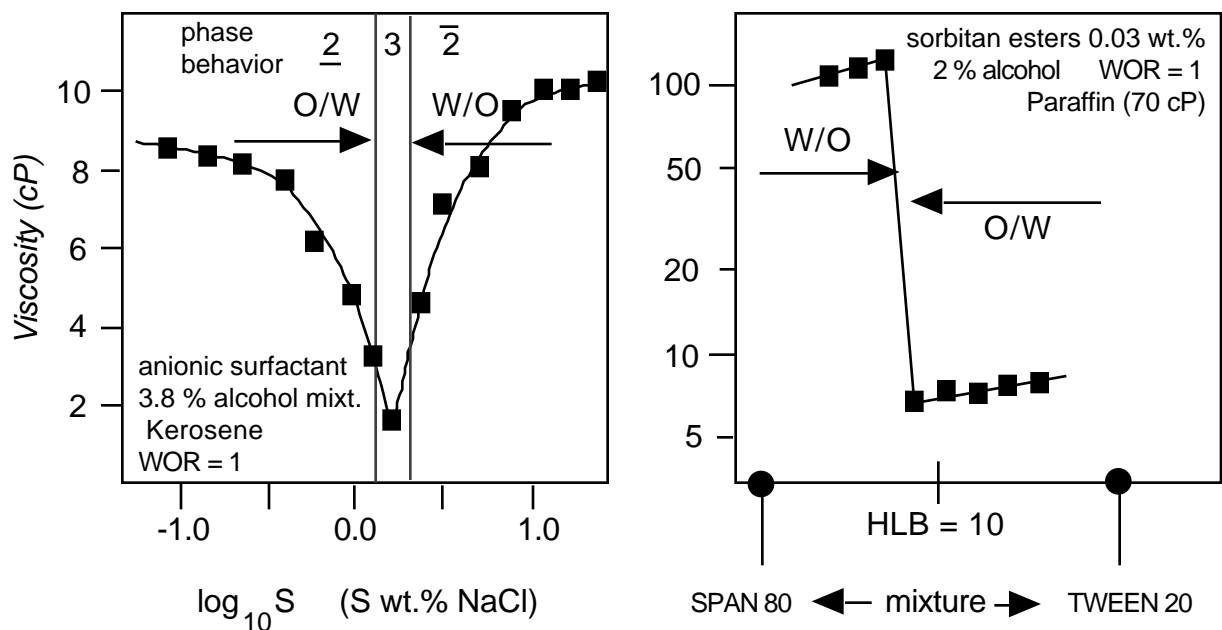


Figure 13: Variation of the emulsion viscosity along a formulation scan. Low viscosity oil (left) and high viscosity oil (right). (After reference 77)

D. Drop Size

The drop size variation is similarly studied along a formulation scan, in which all emulsions are made according to a standard protocol using the same stirring device and conditions (rotational speed and duration). In the following figures the average drop size is the median, but it could be calculated by any of the classical methods with no avail upon the generality of the conclusions.

Figure 14 (right) indicates the variation of the emulsion drop size along a formulation scan, which here is a temperature scan with a nonionic surfactant. Optimum formulation, here optimum temperature T^* , essentially corresponds to Shinoda's phase inversion temperature (PIT) (80) where the surfactant affinity switches from hydrophilic to lipophilic.

Figure 14 (right) indicates that there are two minima in drop size, one at some distance from optimum temperature but below it (O/W) and another one slightly above it (W/O).

The occurrence of these two minima may be interpreted by analyzing the variation of the interfacial tension (Figure 14, left) and emulsion stability (Figure 14, center) along the same formulation scan (81-82). The difference between the two variations is essentially due to the fact that the tension variation takes place over a much wider temperature interval than the stability change. The combination of these two factors that have opposite effects on the drop size generates the shown variation. When optimum formulation is approached (from any side), the first effect to be felt is the tension reduction, which makes breakup easier with a resulting drop size decrease. Then, when the rapid reduction in emulsion stability takes place, the coalescence rate grows very quickly and the trend is reversed to produce larger drops. Consequently, the minimum size drop is not attained at optimum formulation, where the tension exhibits its lowest value, but at some "distance" from it, where the best compromise between low tension and not too unstable emulsions is reached.

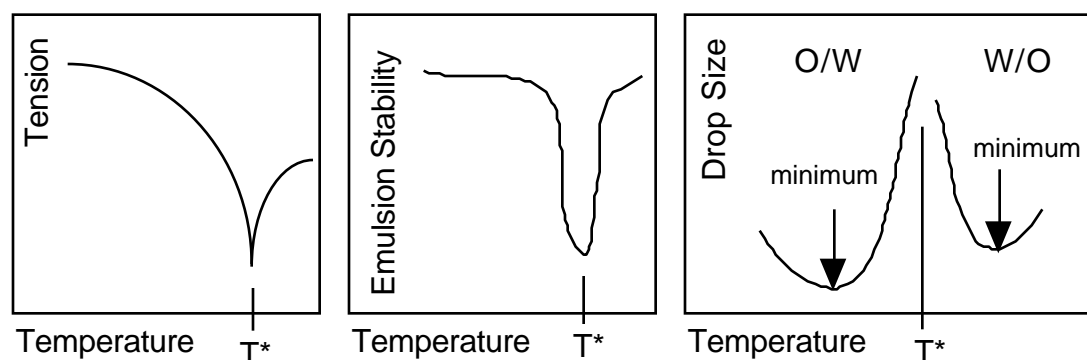


Figure 14: Typical variations of the interfacial tension (left), emulsion stability (center) and emulsion drop size (right), along a formulation scan. Case of nonionic system and temperature scan.

Since the phenomenon takes place when approaching optimum formulation from both sides, there are two drop size minima, on the O/W and W/O sides, respectively. Since the relative strength of antagonist effects may vary from one side of optimum formulation to the other, the drop size variations are not necessarily symmetrical with respect to optimum formulation.

III. FORMULATION/COMPOSITION MAP

A. Crossed Effects on Bidimensional Map

The previously reported dependency of different properties upon formulation is quite general for systems containing similar amounts of oil and water, but it is found to be no longer valid when the internal phase amount increases beyond some value, e.g., 70 or 75%. In such a case the emulsion type and properties are found to also depend on composition. In the simplest ternary case there are two independent composition variables, that are generally taken as the surfactant concentration and the water-to-oil ratio. The crossed effect of formulation and composition would be perfectly visible in diagrams exhibiting a property variation vs. the corresponding variables. For a bidimensional map one variable would be the generalized formulation while the other would be either the surfactant concentration or the water-to-oil ratio.

Although the surfactant concentration plays an important role, it is not the most critical variable, essentially because it is almost fixed by practical conditions. Actually a minimum surfactant concentration, often in the 0.3 wt.% range, is required to attain a satisfactory stability level. On the other hand a too high surfactant concentration, say for instance 15%, would often result in a monophasic system that would not produce an emulsion. In most practical cases the surfactant concentration is limited to a very small percentage just for cost considerations and toxicity constraints.

Accordingly, the bidimensional studies are carried out on a bidimensional map (formulation-water/oil ratio) at constant surfactant concentration and constant stirring with an emulsification protocol, called “standard” emulsification from preequilibrated system, that proceeds as follows. First the surfactant-oil-water system, typically 100 mL, is left to equilibrate in a capped beaker or a similar closed vessel at constant temperature for the duration which is sufficient to attain physico-chemical equilibrium, e. g., 2 or 3 days. The system is then stirred in a turbulent fashion with a turbine blender, for a short time, e. g., twenty or thirty seconds. The turbine blender impeller is almost the size of the vessel, and the rotating speed is high (e. g., 5000 rpm) so that instant mixing is attained. Under such conditions it is found that an extension of the stirring duration would not change the drop size very significantly. The electrolytic conductivity is measured immediately after emulsification to determine the emulsion type. Then, and provided that the emulsion is stable over several minutes, properties such as drop size distribution and viscosity

are evaluated. Stability is estimated by pouring an emulsion sample in a graduated test tube which is then capped and placed in a vertical rack kept in a constant-temperature enclosure. The separated phase volumes are monitored from time to time and the stability is expressed as the time required for some settling percentage to take place, e. g. 50% internal phase separation.

Such experiments are carried out on different points of the bidimensional formulation-WOR composition map to cover the region of interest. Constant grid size coverage is generally not the smartest experimental design policy since it does not minimize the overall task. Several judiciously placed one-dimensional scans, both formulation changes and WOR composition variations, would often produce a much better result, in particular because the variations along a scan may be interpolated, a feature of first importance to buildup the contour map. The iso-property contours are drawn by joining the points with the same value of the property, using interpolation between points as needed. The availability of well-fitted continuous variations of the property along some directions is extremely useful to decide how to fill the gaps. The selection of the proper scans to do so will be discussed after the analysis of the typical features of such a map.

B. Conductivity Map and Emulsion Type

Figure 15 indicates the variations of the emulsion electrolytic conductivity vs. formulation (aqueous phase salinity) at different constant water-to-oil ratios, indicated by the water volume fraction fw (83). When fw ranges from 0.4 to 0.7, the conductivity exhibits the typical pattern, already mentioned in the previous section. Suboptimum salinity ($SAD < 0$) is associated to O/W emulsions, while overoptimum salinity results in W/O ones.

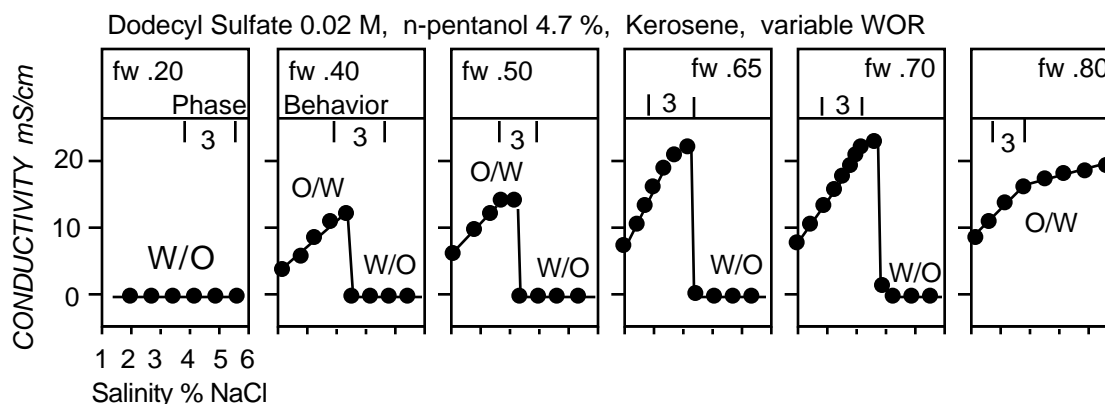


Figure 15: Variation of emulsion conductivity along a formulation (salinity) scan at different water proportions. (After reference 83).

There is however a slight change in the conductivity curves as the water fraction increases, and it is worth remarking the weak shift in the conductivity drop (inversion point) from the extreme left (case $fw = 0.4$) to the extreme right (case $fw = 0.65$ and 0.7) of the three-phase behavior zone.

Whenever fw is lower than some critical value (here 0.3) a low conductivity everywhere indicates a W/O type emulsion, even when the salinity is below optimum (case $fw = 0.2$). On the other hand, at high water content (case $fw > 0.8$) the opposite occurs, i. e., the conductivity remains at a high value, indicating a O/W type emulsion, even when the salinity is above optimum. It is worth noting however that an unambiguous break in conductivity variation is exhibited at optimum formulation (case $fw = 0.8$). Indeed, the conductivity increases with a weaker slope after optimum formulation, an indication that the emulsion is actually not a simple O/W type.

By combining the data from all previous (and other) curves, an iso-conductivity map is constructed as indicated in figure 16 (left). The bold line is the inversion geometrical locus, i. e., the frontier between high (O/W) and low (W/O) conductivity emulsions, which is quite easy to determine according to the shape of the curves.

This line exhibits a stair shape that has been found to be typical of many systems. In the central region (e. g., $0.3 < fw < 0.7$) the inversion line is essentially horizontal, while it exhibits two vertical branches on both extremes. It is fair remarking that this kind of inversion map was mentioned in early work on the phase inversion temperature with nonionic surfactant systems (84), although the vertical branches were not entirely studied.

This is not surprising since the temperature is known to produce a formulation effect on these systems, as fully confirmed recently as far as the bidimensional map is concerned (85).

Iso-conductivity contours at 2, 4, ... 24 mS/cm are plotted in the O/W zone of figure 16 (left). In the central region, these contours are straight slanted lines, because both an increase in salinity and an increase in brine content would roughly result in a proportional conductivity augmentation. In the O/W zone that is located above optimum salinity, i. e., on the upper right of the plot, the iso-conductivity contours appear to be much more slanted. This means that at a given water content, the emulsion conductivity is lower than expected from the typical phenomenology. This is an indication of the existence of a W/O/W type multiple emulsion, which is easily corroborated by microscopic observation. Similarly, the W/O region located in the lower left part of the plot often exhibits a O/W/O type multiple emulsion.

The map has been divided into six regions indicated in figure 16 (right) symbolized by a letter and a sign (83), a setup which has been adopted by other investigators (86-89). The A region corresponds to water-to-oil ratio mid-range, while the B and C regions are associated with low and high water contents respectively.

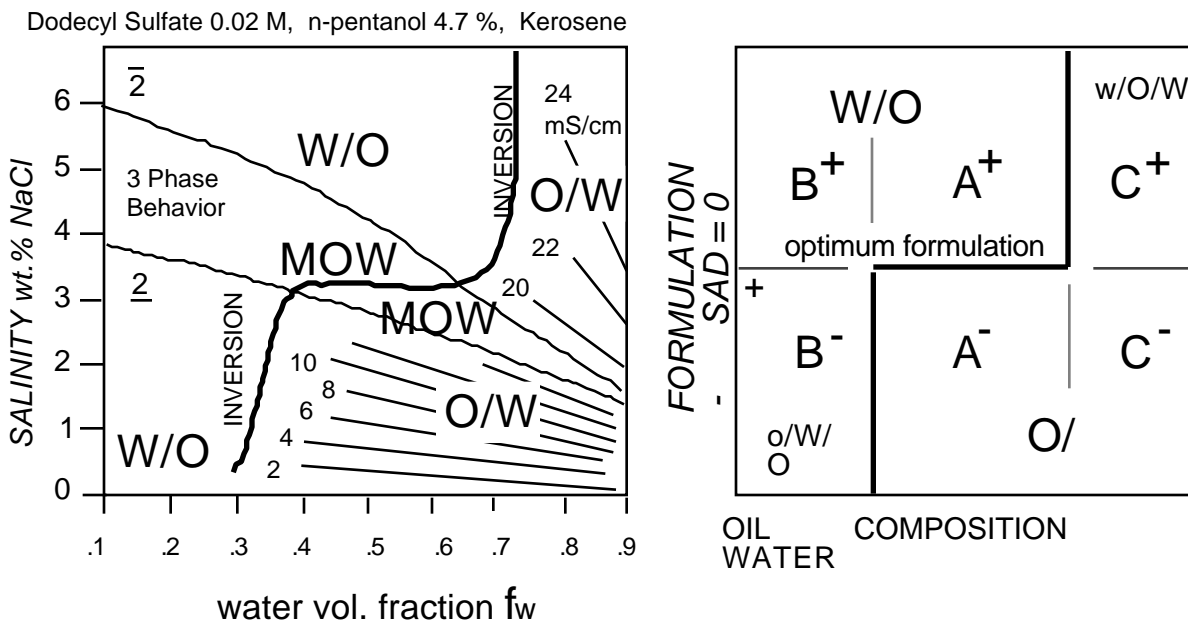


Figure 16: Mixed bidimensional (formulation-composition) map showing the phase behavior at equilibrium and the emulsion iso-conductivity contours (left). Simplified map patterns with inversion locus and region labels (right). (After reference 83)

The frontiers are typically 30 and 70% water, with emulsions containing low viscosity fluids, though they could be quite different in other cases. The formulation effect is rendered through the SAD value sign, i. e., (+) for above optimum situation and (-) for the opposite case.

The A⁻ C⁻ and A⁺ B⁺ are called normal O/W and W/O regions, respectively, because the emulsion type matches the interface curvature expected from phase behavior according to the wedge theory and similar rules of thumb.

B⁻ and C⁺ regions exhibit multiple emulsions, of the O/W/O and W/O/W type, respectively. They are the so-called abnormal regions because the "principal" or "outside" emulsion is not of the type expected from the formulation. Nevertheless, it is worth noting that the most "inside" emulsion, i. e. the small droplets that are located inside the drop of the multiple emulsion, do comply with the curvature requirements set by formulation.

The stair shape of the inversion line may be determined easily by a relatively small number of unidimensional scans. First, one or two formulation scans located from 40 to 60 % water content allow to locate the (formulation position of) horizontal branch of the inversion line. Then, a few composition (f_w) scans located both below and above the horizontal branch allow to locate the position of the vertical branches of the inversion line. Whenever there is no previous information on the system, the first composition scans to be carried out may be located at two or three "formulation distance" units from optimum formulation. These "distances" are evaluated from the correlation for optimum formulation, as discussed at the end of previous chapter. This dual scan technique insures

that the inversion line is found by crossing it perpendicularly, which is of course the most accurate method. The horizontal branch of the inversion line has been associated with the so-called "transitional" inversion, while the vertical branches correspond to the "catastrophic" inversion, a labeling whose origin will become evident later on.

C. Stability Map

The emulsion stability map is constructed in a similar way. Emulsions made from preequilibrated systems according to the standard procedure are left to settle and their stability is measured as the time for some settling, e.g. 50%, to take place. Sufficient measurements should be carried out so that isostability contours might be drawn. As with conductivity measurements a clever location of tested systems according to the expected pattern could greatly improve the experimental yield.

Figure 17 indicates a typical iso-stability map representative of different reported results (2-90). The number typifying each isostability contour is the decimal logarithm of the time (in seconds) to produce a $V_c/V = 2/3$ settling according to the previously discussed method. It is seen that high stability regions are located in the center of the A^- (O/W) and A^+ (W/O) zones, with some extension on the C^- and B^+ normal zones, respectively, with low-internal-phase-ratio emulsions, which are however likely to exhibit creaming-type separation. The stability minimum found near optimum formulation occurs at all compositions, and it appears as an elongated "valley" that closely follows the three phase behavior band, whatever its slanting.

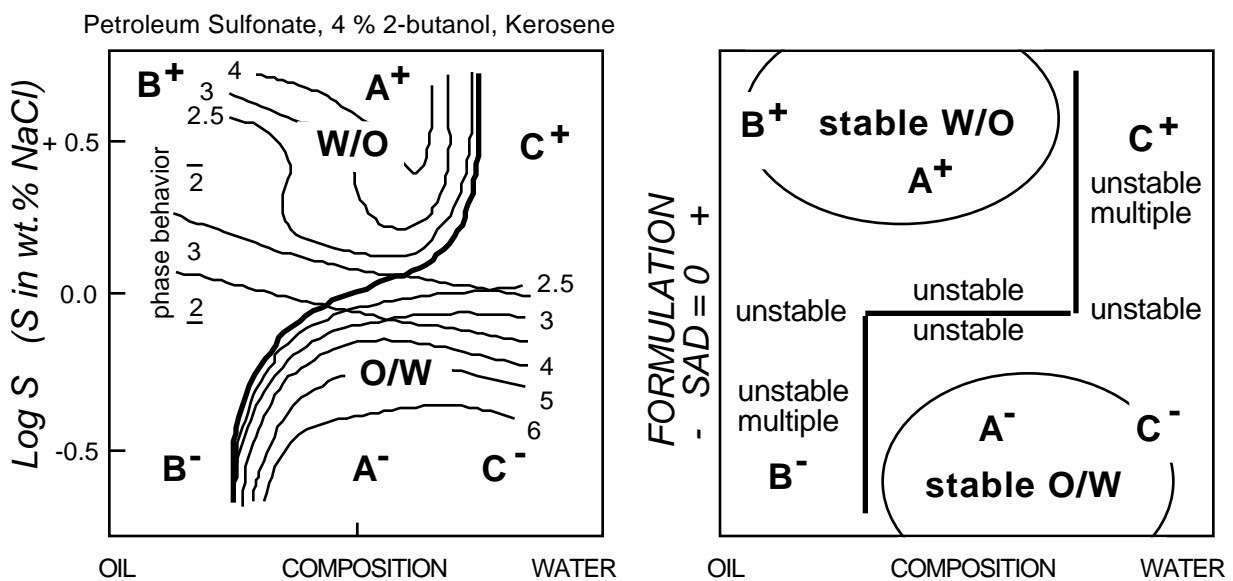


Figure 17: Bidimensional formulation-composition map showing the emulsion iso-stability contours as logarithm of required time (in second) for 2/3 settling (left). After reference (2). Simplified map patterns by region (right).

Abnormal regions C^+ and B^- also exhibit low-stability emulsions, a feature which is consistent with the fact that the emulsion type and thus interface curvature, is opposite to the one favored by the formulation effect. Since multiple emulsions are often made in these regions, a closer look is warranted. For instance a multiple $W_1/O/W_2$ emulsion is found in the C^+ region. W_1 represents the most internal phase, i. e., the water droplets that are located inside the oil drops. It may be considered that the "principal" or "outside" O/W_2 emulsion has the W_1/O "inside" emulsion as internal phase. Since the W_1/O "inside" emulsion matches the expected type from formulation effects, it is certainly stable, whereas the outside emulsion is not. Thus, such a $W_1/O/W_2$ emulsion would quickly decay in a two layer system, consisting of a W_2 phase and an oil layer that would actually be a W_1/O emulsion, which is expected to be quite stable if the formulation is sufficiently away from optimum. This means that such "unstable" multiple emulsions are not necessarily yielding a quick and complete phase separation, unless the formulation is appropriate, e. g., near optimum. This feature could be useful for applications dealing with controlled release or capture through mass transfer.

It is obvious that a multiple emulsion would be fully stable only if both inside and outside emulsions are stable at the same time. From the previous results it is clear that only one of the inside or outside emulsions may be stabilized by a surfactant at equilibrium according to any repulsion mechanism. Hence, the other emulsion has to be stabilized by some other effect, generally a dynamic one. For instance, in the stabilization of a $W_1/O/W_2$ multiple emulsion, the A^+ region may be selected to formulate first the W_1/O emulsion, e. g., with a lipophilic surfactant called LS. Then the W_1/O emulsion is poured into a vessel containing W_2 phase under constant stirring, so that a O/W emulsion may be made. If a hydrophilic surfactant (called HS) is dissolved in W_2 to stabilize the O/W_2 emulsion, in which O is really the inside W_1/O emulsion, then the system ends up containing two surfactants, LS and HS. These two surfactants will conceivably migrate to both W_1/O and O/W_2 interfaces, and equilibrium will be reached after some time, so that the same mixture of LS and HS will be present at both interfaces. Since this mixture cannot be simultaneously lipophilic and hydrophilic, it will not stabilize both emulsion types but only one of them. The trick (91) is to avoid the migration of the second (HS) surfactant from the W_2 phase to the W_1-O interface, and as a second priority, the migration of the LS surfactant from W_1-O interface to $O-W_2$ interface. This is attained by using an HS surfactant with a very slow desorption rate, e. g., a polymeric substance that possesses several lipophilic and hydrophilic groups. Such amphiphilic polymers are attached to the interface by several "plugs", so that the desorption requires the unplugging of all attachment points at once, which is extremely unlikely. Moreover, the HS polymeric surfactant may be selected to be quite hydrophilic with a very low solubility in the oil phase, so that the transfer through it is improbable.

The close examination of typical maps indicates that the most stable emulsions are not found always at the center of the corresponding A region, but sometimes rather on the side of the vertical branch of the inversion line, i. e., towards the high internal phase ratio region. However, this trend may be misleading as far as its interpretation is concerned. In effect, an increase in internal phase content often results in a change in viscosity and drop size for a given stirring procedure, which could be the actual justification for the stability change.

Depending upon the case, the high stability region is very limited in area or extends quite away from optimum formulation. In any case, the stability is often found to decrease far away from optimum formulation, because the surfactant becomes too hydrophilic or too hydrophobic.

D. Viscosity Map

The viscosity map is in general simpler than the stability one, probably because the emulsion viscosity is quite directly related to formulation and composition. In effect, in both A regions the viscosity decreases as optimum formulation is approached, and augments as internal phase content increases. As a consequence the isoviscosity curves follow the inversion line as indicated in Figure 18. The highest (relative) viscosity zones are located near the vertical branches of the inversion line, inside the A regions, where the effect of the internal phase ratio increase is enhanced by the occurrence of the smallest drop size for a given stirring process (see next section).

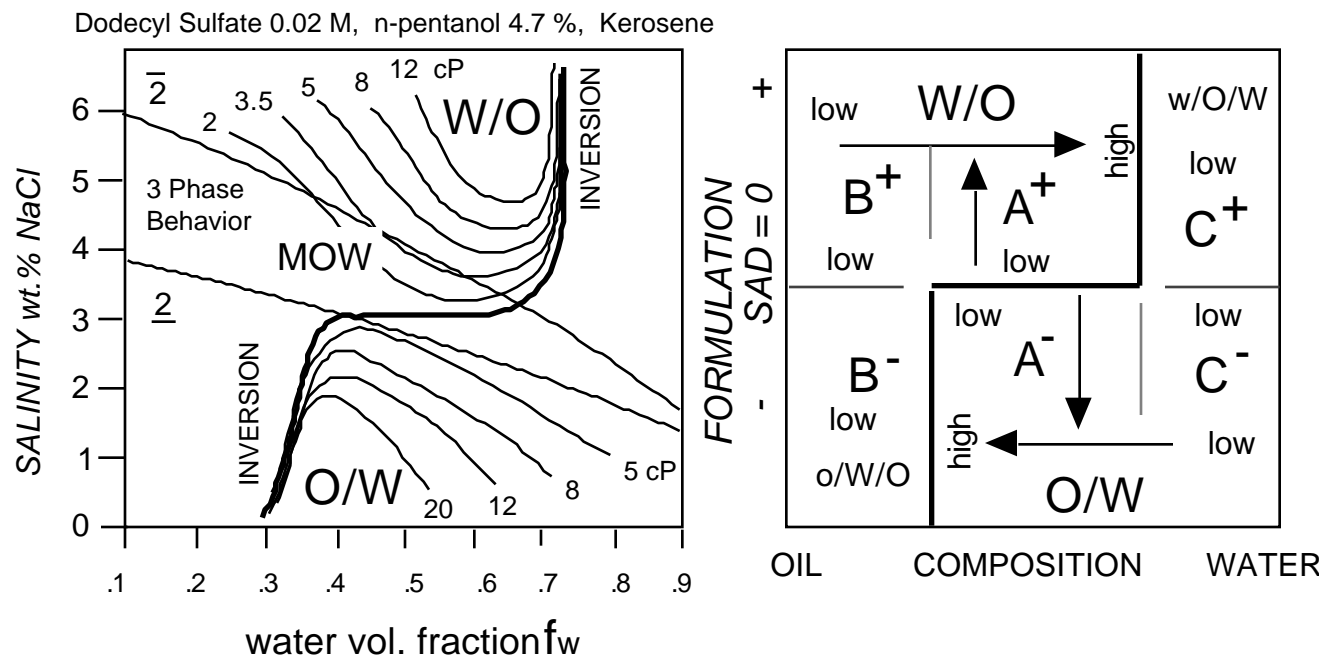


Figure 18: Bidimensional formulation-composition map showing the emulsion iso-viscosity contours (left). Simplified map patterns indicating viscosity increase in the direction of arrows (right). After reference (2)

The arrows in figure 18 (right) indicate the directions of increasing viscosity at constant formulation (horizontal) and constant composition (vertical). It is worth remarking that when the inversion line is trespassed across the horizontal branch, the viscosity undergoes through a minimum, whereas it proceeds through a maximum when any of the vertical branches is crossed.

Low-viscosity emulsions are found in the vicinity of optimum formulation or in the low-internal-phase-ratio regions B^+ and C^- . Besides these general trends, it is of course important to remember that the viscosity may be modified as well, by changing the continuous phase viscosity and the drop size average and distribution.

E. Drop Size Map

The emulsion drop size depends upon such a high number of different variables that it is difficult to separate and impute all effects. In what follows a standard emulsification protocol is applied to a preequilibrated system, so that the change in drop size is only due to formulation or composition effects, or their direct consequences on other properties such as tension, stability and viscosity. In fact very few maps have been experimentally determined and only trends are available (81, 92).

The complex formulation effect previously discussed is found in all cases studied, whatever the formulation variable. Hence, the minimum drop size is attained at some "formulation distance" from optimum in both A regions, as schematically indicated in figure 19. However, the exact position of this minimum strip depends upon stirring conditions and physicochemical properties.

The composition effect is not simpler. It has been found with low-viscosity oil/water emulsions that the drop size tends to first increase then decrease as the internal phase ratio increases (93). This results in isodrop size contours as indicated in figure 19. On the other hand it seems that with high viscosity oil, the drop size steadily decreases when the internal phase ratio increases. It is important to remark that in both cases, the drop size decreases considerably when approaching the inversion line by augmentation of the internal phase content in any A region (a path indicated as a black arrow). This effect seems to be due to a considerable improvement in stirring efficiency in the viscous high-internal-phase-ratio emulsions located in these zones. So far, it is not known whether this fact is absolutely general, but it may be said that it is a quite common circumstance, and this is why figure 19 indicates the presence of a small drop size strip in the vicinity of the vertical branches of the inversion line.

F. Effect of Other Variables on the Inversion Line

In many maps, the property contours nearly follow the inversion line which exhibits a horizontal branch and two vertical branches. Actually the "horizontal" branch is not necessarily horizontal,

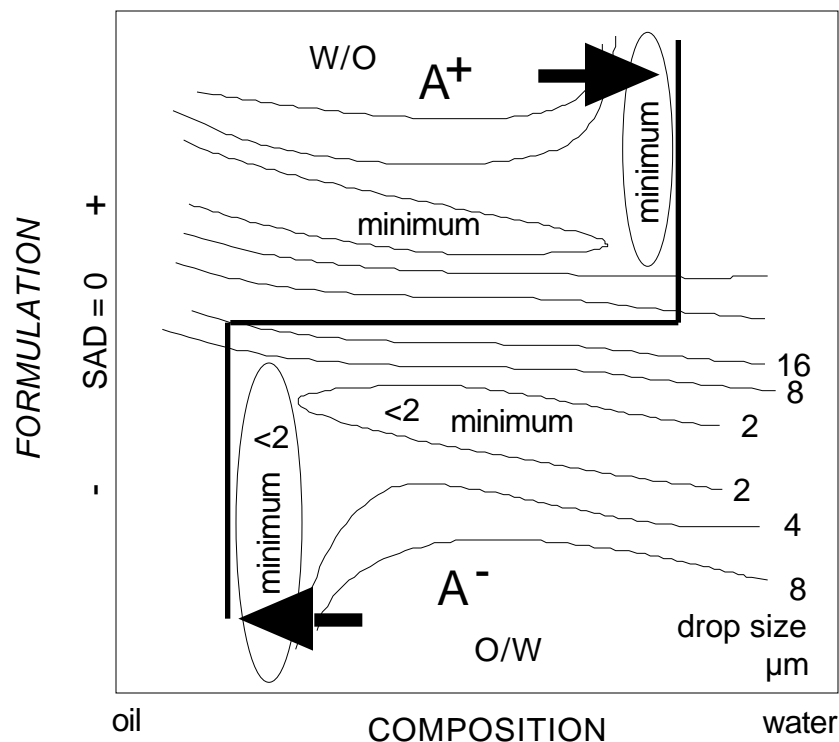


Figure 19: Scheme of a bidimensional formulation-composition map showing the most probable emulsion iso-drop size contours. (After reference 93)

but it always closely follows the three-phase or optimum formulation strip in the middle of the diagram. In some cases the optimum formulation strip is found to be quite slanted, i. e., optimum formulation changes when the water/oil composition changes. This slanting seems to occur only with surfactant mixtures or surfactant-alcohol mixtures that exhibit the so-called fractionation phenomenon. This has been studied thoroughly (94-97) but is too complex to be exposed here in detail, and it will be only treated qualitatively.

The basic rationale is that when a surfactant-oil-water system contains two (or more) surfactant species with quite different hydrophilicities, the species partition into the two phases and at interface (or in the middle phase microemulsion) in different ways. For instance, for nonionic surfactant (commercial) mixtures, many of the most lipophilic oligomers partition into the oil phase, while the migration into the aqueous phase is severely limited by the critical micelle concentration, and is hence essentially negligible. Consequently, the interface (or microemulsion) contains the remaining oligomers that are more hydrophilic than the mixture average. Thus, it may be said that when fractionation occurs with nonionic surfactant mixtures, the interface composition is more hydrophilic than the overall or global composition. Since it is known that at optimum formulation, the amphiphile hydrophilicity at interface is fixed whenever the oil, water, and temperature are fixed, it is actually equivalent but preferable to state than the overall composition is more lipophilic than the interface composition. It has been shown that when the composition variables (surfactant

concentration and water/oil composition) change, the partitioning changes, so that a constant interfacial hydrophilicity mixture requires a changing overall hydrophilicity. This is why the apparent or global formulation (e. g., mixture EON) changes with the water/oil composition as indicated by the slanting.

The importance of this phenomenon increases with the difference in hydrophilicity of the surfactant and alcohol species present in the amphiphilic mixture. It is found to be almost negligible with pure ionic surfactants, even in the presence of intermediate alcohols (sec-butanol). It increases slightly when a surfactant and an alcohol of very different hydrophilicities are used, e. g., sodium dodecylsulfate and pentanol. It is most significant and essentially unavoidable with commercial ethoxylated nonionic surfactants, particularly the low ethoxylation ones (EON < 10) that contain oligomers with extremely different hydrophilicities. Figure 20 shows such a case in which the optimum formulation region (shaded) is extremely slanted. It is worth remarking that in this case, the strong slanting which could be normally attributed to the nonionic surfactant mixture partitioning, is exacerbated by the presence of a lipophilic alcohol such as n-pentanol (2).

The fractionation and the resulting slanting of the horizontal branch is enhanced when the surfactant concentration decreases. As a rule of thumb, it may be said that the effect is moderate at or above 3% surfactant, while it becomes dominant below 0.5% surfactant, and quite worrisome below 0.1%. In any case the slanting of the horizontal branch may be easily detected by carrying out two formulation scans near the map center, for instance at 30 and 60% water. As far as the property mapping is concerned, it is only necessary to distort it according to the slanting. This may of course produce some unusual situations as seen in Figure 20, where a rather small A^+ region is

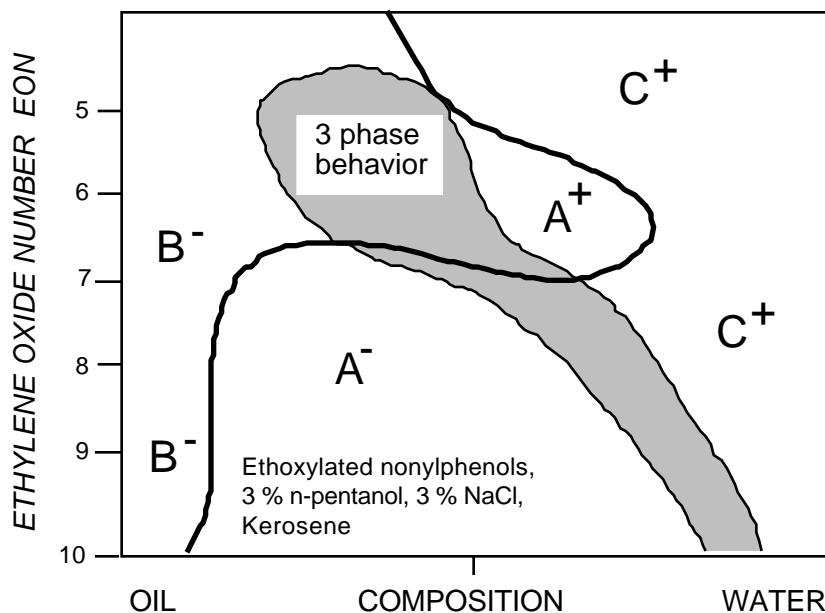


Figure 20: Bidimensional formulation-composition map, showing the emulsion inversion locus, in case of strongly slanted optimum formulation band. (After reference 2)

squeezed in between the very slanted optimum formulation zone and a A^+/C^+ vertical branch normally at 50% water. In such a case it is clear that the occurrence of stable W/O emulsion (associated with A^+) is restricted to a very small zone in the map.

The vertical branches of the inversion line have been found to depend on most of the other variables that are susceptible to participate in the balance of breaking and coalescence rates occurring during emulsification. No exhaustive information is available at the date but some trends have been found (83, 98).

First to be detected was the effect of the phase viscosity at constant stirring energy. When the oil phase viscosity increases, it is found that the A^+/C^+ branch is shifted to the left, thus reducing the extension of the A^+ zone, where the oil phase is the external phase. Meanwhile the location of the A^-/B^- branch is essentially unchanged. The effect may be so drastic that the A^+/C^+ (right) branch can be shifted to 20 or 30% water, i. e., eventually to the left of the (left) A^-/B^- branch, with extremely viscous oil phases.

Exploratory investigations indicate that when the water phase viscosity is increased, e. g., by adding a polymer, then it is the A^-/B^- branch which is shifted, this time to the right (93). It may be said as a general statement that when the viscosity of one of the phase increases, the extension of the region where this phase is the external phase of a normal stable emulsion is reduced. In other words, when the viscosity of a phase increases it is more difficult to make emulsions in which this more viscous phase is the external phase. This is quite consistent with the well known experimental fact that when two liquids are stirred (in absence of surfactant), the most viscous liquid turns out to be dispersed into the less viscous one.

As far as the effect of stirring is concerned, it is found that not only the energy but also the kind of stirrer could be quite important, keeping in mind that the most vigorous stirring is not the one that would necessarily lead to the smaller drop size. When working with a rotational stirrer and changing the speed, it has been found that increased stirring energy tends to shift both vertical branches towards the center of the map (99), and hence to reduce the extension of both A^- and A^+ zones, as if increased stirring were offsetting the formulation effect (central zone), and favoring the composition influence, i.e., the formation of an emulsion in which the most abundant phase is the external phase and vice versa (extreme zones). Note that this rectifies a misleading statement on the subject in a recent review (100), which otherwise sums up the state of the art on the topic.

An increase of surfactant concentration is found to produce the opposite effect, i. e. both vertical branches are shifted towards the extremes and the A zone range extends (101). This is actually not surprising since an increase in surfactant concentration should logically favor the effect of formulation. It is worth noting that an increase in surfactant concentration is also associated with

a decrease in drop size in most cases (82), because of an improved coalescence inhibition, at least below the critical micelle concentration (3).

Judicious logical reasoning may be carried out by combining these effects. For instance, if a W/O high internal phase ratio emulsion is to be made with a viscous oil, then it is favorable to decrease the stirring energy and to increase the surfactant concentration. An alternative would be to increase the temperature to reduce the oil viscosity, provided that the corresponding formulation effect is not detrimental (as could happen with ionic surfactants). Actually such situations can be solved also by using the memory feature discussed in the next section.

IV. DYNAMIC PHENOMENA IN EMULSION MODIFICATION

In the preceding sections, emulsions were prepared from preequilibrated surfactant-oil-water systems, and their properties were sufficiently persistent that they did not change significantly during the time scale of the measurement or the application. This is not always the case, and it is not uncommon practice to modify the emulsion formulation or composition according to some procedures involving a temperature variation, a continuous or lump addition of one or two phases with or without surfactant, and/or a changing stirring method, sometimes according to some whimsical protocol. Since these changes are likely to modify the location of the representative point of the system in the bidimensional map, with a corresponding change in property, the question is to know whether the maps are still useful to predict the emulsion property evolution along the path, and when and how this can be done.

The problem may be split into two cases. The first one deals with a modifying path that does not trespass through the map inversion line, in which case it is often possible to make a good forecast concerning the property alterations. This is not the case whenever the inversion line is crossed over. In some cases, the dynamic crossing of the inversion line defined previously does not trigger the inversion, which is somehow delayed, and some "guesstimate" may be advanced. However, if the change proceeds, sooner or later the inversion would take place and a completely new emulsion would be formed through a chaotic transition. There are two types of emulsion inversions and in spite of some clever fundamental hints (89, 102), in none of them it is known for sure what happens at the very moment of inversion. Nevertheless, the transient phenomena taking place during the inversion have been advantageously harnessed to produce handy systems such as miniemulsions.

A. Modifying Emulsions Without Inversion

In this section it is assumed that a so-called initial emulsion is made from a preequilibrated surfactant-oil-water system located at some "initial" point in the bidimensional map, with properties

corresponding to its position in the map. Then a change that may affect its formulation and/or composition is applied to the emulsion, so that the representative point is shifted to another place in the map located on the same side of the inversion line. The final "shifted" emulsion corresponds to a point on the map, in which the corresponding standard emulsion exhibits other properties. The question is whether the "shifted" emulsion keeps its "initial" properties or embraces the "new" ones that correspond to its final position in the map.

Since it may be generally assumed that the change duration is quite short, the answer is often elemental and utterly rational, simply because some properties are maintained during the formulation and/or composition change while others are not.

Provided that the emulsion remains stable over the change, the drop size stays constant, as well as other related properties. If the internal phase content is increased by adding some amount of this phase (under constant stirring), as along path 1 in Figure 21, emulsion viscosity is expected to augment from the increase in internal phase content, although other effects would have to be taken into account, such as the efficiency of the stirring required to proceed with emulsification of the added internal phase, or the eventual production of a bimodal distribution that could result in a viscosity reduction.

If the formulation or temperature is changed so that the emulsion representative point is shifted from a high stability region to a low stability one, as for instance by approaching optimum formulation as along path 2 in Figure 21, the emulsion accelerated decay becomes the main concern and drives other property changes like drop size growth and viscosity abatement. Path 2 is thus advised when emulsion breaking is sought.

Some composite path could take advantage of different helpful features, as in case (3), where the initial emulsification is carried out "at some distance" from optimum formulation where

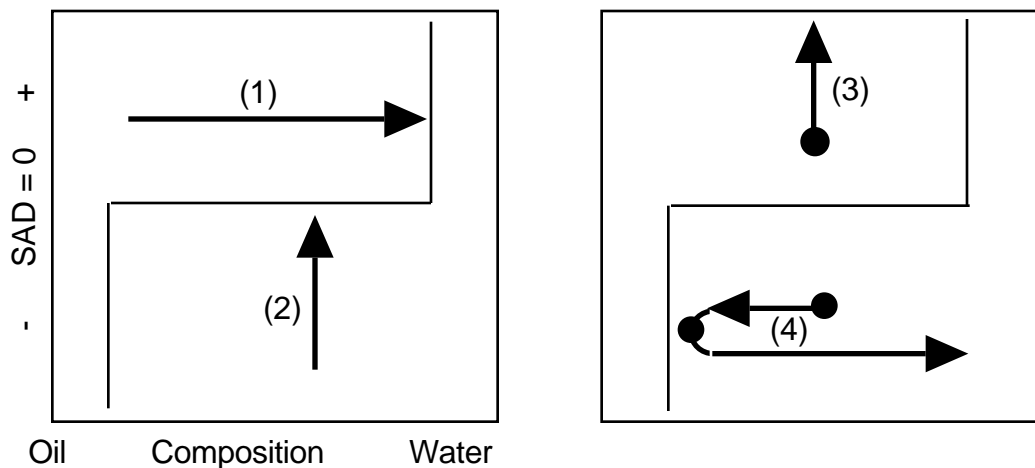


Figure 21: Emulsion dynamic changes that do not trespass the inversion locus

the smallest drop size is expected (black circle at the start of path 3 in figure 21), although it is too near optimum formulation to exhibit a satisfactory stability. In order to counter this dilemma, the formulation or temperature is changed quickly after emulsification, so that the representative point moves away from optimum formulation until a high stability is secured. This method was suggested quite a long time ago under the name PIT emulsification method (103), where the selected formulation variable is the temperature. Note that it could be carried out with any formulation variable that may be changed quickly through a lump addition of matter, e. g., surfactant hydrophilicity, alcohol contribution, salinity increase.

Path 4 illustrates an even more complex way to produce a very fine drop emulsion with a low internal phase ratio, e.g., 1:5, as in a make up removal milk. At such low internal phase ratio, the emulsification is very inefficient and energetically expensive, and it is quite painstaking to produce a monodispersed fine emulsion even with a colloid mill. This obstacle is circumvented by the following procedure. A starting medium drop size emulsion with approximately 50-60% internal phase proportion is shifted to high internal phase content until the vicinity of the inversion line is attained, say, at 80%. Proceeding this way, there is generally no danger to trigger the inversion for the reasons discussed in the next section. The viscosity becomes quite high in this region, but a slow-motion whip-style stirring turns out to be very efficient and extremely small droplets can be produced with little expense of energy. When the fine high-internal-phase-ratio emulsion is finally made, it is then diluted with a large amount of external phase to match the required 20% internal phase composition. Often a slight formulation change is additionally applied to enhance the stability of the final emulsion, although the extremely small drop size could be sufficient to considerably slow down the creaming kinetics.

B. Emulsion Dynamic Inversions and Applications

Up to now the inversion line has been the limit between emulsion types when emulsification is carried out from a preequilibrated system according to the so-called standard procedure. In practice the emulsion inversion could also be the situation in which a change in formulation or composition triggers a switch in emulsion type. This kind of inversion is generally called dynamic inversion since it takes place as a consequence of the change. Depending on the circumstances it may be favorable or quite detrimental, and should be either harnessed or avoided.

Dynamic inversion is studied by producing a change that moves the point that represents the formulation and composition of an emulsion on the map from one side of the inversion line to the other side. In practice the system is first equilibrated and then emulsified, to produce the initial emulsion. Then, its formulation or composition is altered continuously or by small increments, while a low-energy stirring is maintained to keep the emulsion from settling, until inversion is

detected, usually by conductimetry. It is worth noting that the stirring should be much less energetic than the one applied to make the emulsion in the first place.

Figure 22 indicates the typical patterns found in dynamic inversion. The arrows indicate the direction and path of change while their respective heads indicate the inversion point along a formulation (white) or composition (black) shift. Depending on which branch is crossed, one of two possible inversion types is encountered.

When a vertical crossing of the inversion line is carried out (white arrows in Figure 22 left), it is seen that the inversion takes place exactly at the same location, i. e., at optimum formulation, whatever the direction of change. Because of these reversibility characteristics, this inversion has been termed "transitional".

The dynamic inversion through any of the vertical branches of the inversion line is quite different. At both crossing boundaries (A^-/B^- and A^+/C^+) the composition is changed so that the emulsion internal phase ratio increases in the direction in which inversion takes place (black arrows). From A^- to B^- and from A^+ to C^+ , it is from a normal emulsion to an abnormal one (left), while from B^- to A^- and to C^+ to A^+ , it is the opposite case (center). Figure 22 indicates that the inversion location depends upon the direction of change. Actually there is a region (shaded) in which the two types of emulsions can be found depending upon the direction of change, i. e., depending upon the previous history of the emulsion, which is why the term "emulsion memory" has been proposed. Everything happens as if the inversion were delayed along the path of change, with the resulting displacement of the inversion line over the shaded region, a phenomenon which was first noticed quite a long time ago (104).

These regions, known as hysteresis regions, exhibit a triangular shape, so that they vanish at optimum formulation, whereas they become wider as formulation departs from optimum. The standard inversion line discussed in the previous section is located somewhere inside the hysteresis region, not necessarily in the middle.

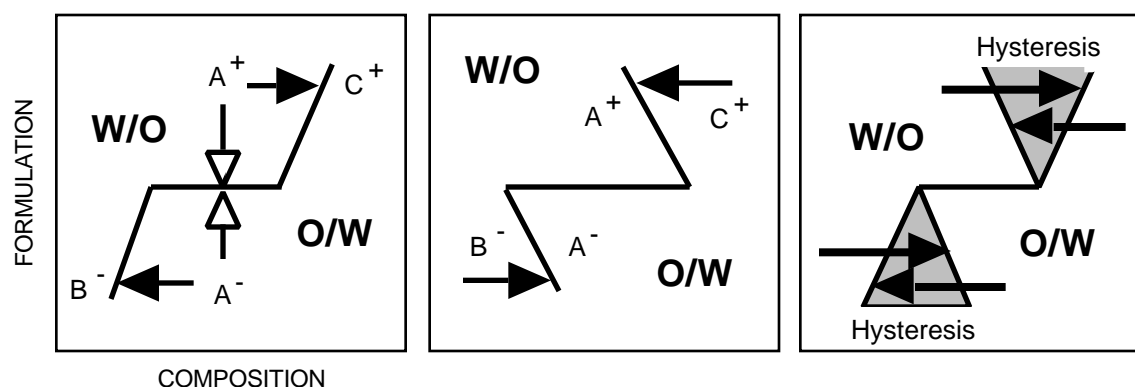


Figure 22: Dynamic changes that produce the emulsion inversion. (After reference 100)

This second type of inversion has been called "catastrophic", for its characteristic phenomenology, similar to the cusp as well as to the higher degree catastrophes (105-109) that have been used to interpret it in a quite satisfactory way, as discussed in a review (107).

In such an inversion, everything happens as if the internal phase ratio could be increased beyond the value corresponding to the standard inversion, with this extra increase being greater as formulation departs from optimum. This feature is of course very useful in practice and was used long ago, e. g., in mayonnaise making, in which oil is added little by little to an aqueous phase containing a surfactant (egg yolk). In this case an A^- emulsion is displaced to the left far beyond the point where an oil-egg yolk mixture results in an egg yolk dispersion in oil by standard emulsification. It is worth remembering that when the internal phase content reaches 70 or 80% the emulsion becomes so viscous that conventional turbulent stirring does not work anymore to incorporate more internal phase. Instead, a slow motion blender is preferred, like a whipping device or a ribbon moving gear, which are often much more efficient. In such a high-internal-phase-ratio inversion scheme, the external phase is stretched as interdrop films, that finally break into small droplets by capillary instability.

It was mentioned earlier that the B^- and C^+ regions often exhibit multiple emulsions, which is actually the simultaneous occurrence of both emulsion types. There is some evidence that multiple emulsions start occurring before the catastrophic inversion takes place, and some researchers have proposed a competitive kinetic model in which one of the emulsions could be more stable and thus would prevail (87, 89, 110). This is consistent with the fact that the variables susceptible to influence the breaking-coalescence mechanisms do influence the location of the inversion line and hysteresis region.

The concomitant occurrence of both types of emulsions near the catastrophic inversion has been used to make extremely fine emulsions, that are often wrongly labeled microemulsions by manufacturers of antifoaming suspensions, floor wax, as well as cosmetics and pharmaceuticals. This occurs when an (unstable) abnormal emulsion is inverted into a (stable) normal one as illustrated in Figure 22 (center). For instance, an abnormal W/O emulsion of the B^- type may be inverted by adding water (containing an hydrophilic surfactant) up to some moderate value, e. g., 40 or 50%, sometimes less if the oil phase is viscous and the surfactant concentration is high. Assume that an $O_1/W/O_2$ multiple emulsion occurs in the B^- region as the B^-/A^- boundary is approached. If an increasing number of extremely fine O_1 drops are formed inside the water drops of a W/ O_2 emulsion just before the inversion, the apparent water drop volume (O_1+W) may become much higher than the real water content (W), and a high-internal-phase-ratio inversion scheme may take

place. In such a case the O_1 oil droplets that were trapped in the water drops are brought together to the ones coming from the (O_2) external oil film capillary instability. As a matter of fact the drop size attained by this process could be considerably smaller than the one that would be reached by intense turbulent stirring.

Enhanced emulsification efficiency along a $B^- A^-$ path can be reached by dissolving the hydrophilic surfactant inside the original oil phase. As water is added the surfactant transfers from oil to water as soon as the fluids are in contact. This transient phenomenon often triggers a spontaneous emulsification which results in extremely small oil droplets. This is, however, too complex an occurrence to be properly interpreted with the formulation-composition map features.

On the other hand, transitional inversion is used as well to attain extremely small drop emulsions, sometimes referred to as miniemulsions or gel emulsions, because of the high viscosity resulting from the exceedingly small drop size, even at low internal phase ratio (111-115).

The formulation transition is in most known cases carried out by changing the temperature with a nonionic surfactant system. According to the previous chapter, an increase in temperature is can modify the phase behavior from Winsor type I to type II for nonionic surfactant systems (or vice versa for ionic ones) undergoing type III (three-phase) or type IV (single-phase) case at optimum formulation as indicated in Figure 23.

Each phase behavior type is associated with an emulsion type, but near optimum formulation either a monophasic (microemulsion) or triphasic (microemulsion at equilibrium with excess oil and water) is exhibited, depending on the amphiphile surfactant/alcohol mixture (S+A) concentration.

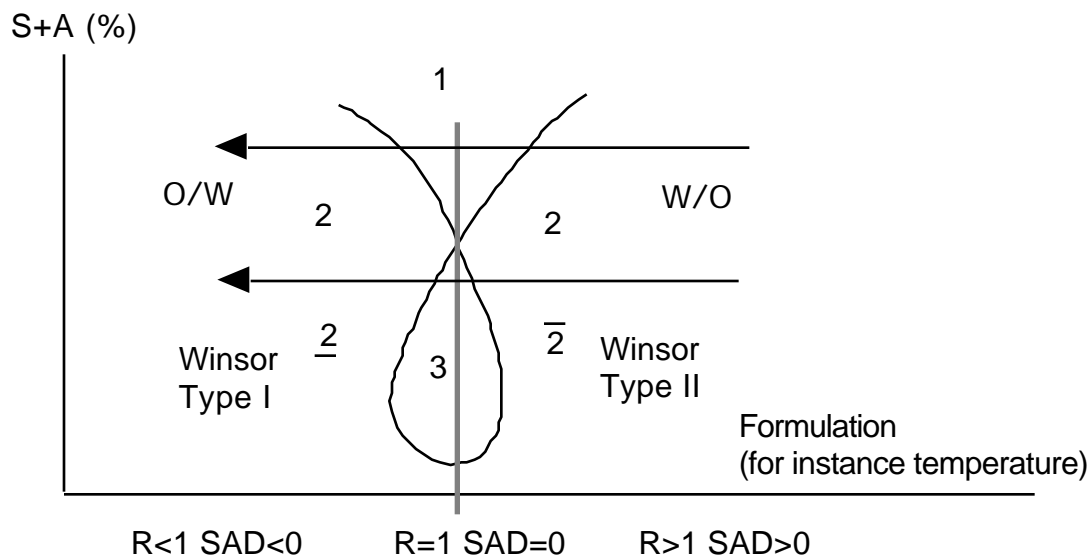


Figure 23: Phase behavior chart as amphiphile amount vs. formulation. Black arrows indicate the paths undergone by emulsified systems physicochemical state as temperature is decreased (nonionic surfactant)

When temperature is changed near optimum formulation, the microemulsion composition changes from mostly oil (type II side) to mostly water (type I side) or vice versa. When this change takes place, the microemulsion tends to exude oil or water droplets as in a nucleation process. If the change in temperature is slow, the droplets have the time to gather and to instantly coalesce, since the emulsion stability is at its minimum. However, if the temperature is very quickly changed after the nucleation takes place, the droplets may be prevented from coalescing and a quenched miniemulsion is formed. The V-shaped single phase region (1) in Figure 23 often displays liquid crystalline phases, that may perform a determinant role in stabilizing the formed droplets, at least by preventing an early coalescence before quenching takes place (74, 116-117).

This mechanism implies that all the oil and water are solubilized into a single-phase microemulsion at optimum formulation. This requires either high solubilization or a high surfactant concentration, and sometimes both, which might not be practical.

If there is not enough surfactant to produce a single-phase system at optimum formulation, some of the emulsion drops will not come from desorption but will be the result of the stirring process, and it would be important to take advantage of the presence of a most favorable compromise in drop size at some distance from optimum formulation (see Figure 14). If the formulation or temperature is adjusted at the minimum drop size compromise and then a quench is applied to quickly shift the formulation from the unstable region, a small drop emulsion may be attained with extreme facility. Nevertheless, it is worth pointing that no miniemulsion can be made this way or by any other way involving stirring emulsification, except when a dynamic inversion process either transitional or dynamic does take place.

Recent research has unveiled that the location and shape of the catastrophic inversion hysteresis zones depend upon other variables, such as stirring, phase viscosity or surfactant concentration, in a way which is consistent with the shift of the standard inversion line vertical branches with these variables (99, 118). For instance it has been found that an increase in surfactant concentration tends to shift the hysteresis regions towards the extreme and to increase their extension (101). Increased stirring energy does just the opposite effect (99), and it could be conjectured that infinitely energetic stirring would result in the vanishing of the hysteresis zone into the standard inversion line.

ACKNOWLEDGMENTS

The author wishes to thank the local and national Research Councils, CDCHT-ULA and CONICIT, for supporting the Lab. FIRP research program at Universidad de Los Andes.

REFERENCES

1. P Becher, *Emulsion: Theory and Practice*, Reprint, R. Krieger, Huntington (1977)
2. M Miñana-Pérez, P Jarry, M Pérez-Sanchez, M Ramírez-Gouveia, J L Salager, *J. Dispersion Sci. Technol.*, 7: 331 (1986)
3. S Rehfeld, *J. Colloid Interface Sci.*, 24: 358 (1967)
4. S Nagata, *Mixing: Principles and Applications*, Wiley, New York (1975)
5. A M Ali, H H S Yuan, D S Dickey, G G Tatterson, *Chem. Eng. Commun.*, 10: 205 (1981)
6. T P Chang, Y H Sheu, G B Tatterson, D S Dickey, *Chem. Eng. Commun.*, 10: 215 (1981)
7. G B Tatterson, *Fluid Mixing and Gas Dispersion in Agitated Tanks*, MacGraw Hill, New York (1991)
8. T Allen, *Particle Size Measurement*, Chapman and Hall, London (1975)
9. M J Groves, *Particle Size Analysis*, Heyden, London (1978)
10. Th Tadros, B Vincent, in *Encyclopedia of Emulsion Technology*, P Becher, ed., vol. 1 Chap 3, M. Dekker, New York (1986)
11. J Sjöblom, ed., *Emulsions and Emulsion Stability*, M. Dekker (1996)
12. G V Jeffreys, G A Davies, in *Recent Advances in liquid/liquid extraction*, C Hanson. ed., p 495. Pergamon Press, New York (1971)
13. B J Carrol, in *Surface and Colloid Science*, E Matijevic, ed., 9: 1. Wiley Interscience, New York (1976)
14. H Hadamard, *Comptes Rendus Acad. Sci. Paris*, 152: 1975 (1911)
15. V Levich, *Physicochemical Hydrodynamics*, Prentice Hall, Englewood Cliffs (1962)
16. K J Lissant, ed., *Emulsions and Emulsion Technology*, 2 vol., M Dekker, New York (1974)
17. D Melik, H S Fogler, in *Encyclopedia of Emulsion Technology*, P Becher, ed., vol. 3: 1, M Dekker, New York 1988
18. H Wang, R Davis, *J. Colloid Interface Sci.*, 159, 108 (1993)
19. X B Reed, E Riolo, S Hartland, *Int. J. Multiphase Flow*, 1: 411 and 437 (1974)
20. A D Barber, S Hartland, *Can. J. Chem. Eng.*, 54: 279 (1976)
21. I B Ivanov, T T Traykov, *Int. J. Multiphase Flow*, 2: 397 (1976)
22. T T Traykov, E D Manev, I B Ivanov, *Int. J. Multiphase Flow*, 3: 485 (1977)
23. D T Wasan, A Nikolov, *First World Congress on Emulsion*, Paris, Oct. 1993. *Proceedings* 4: 93 (1993)
24. I B Ivanov, P A Kralchevsky, *Colloids Surfaces A*, 128: 155 (1997)
25. A W Adamson, *Physical chemistry of Surfaces*, 3rd Ed., Interscience, New York (1976)
26. M Rosen, *Surfactants and Interfacial Phenomena*, Wiley, New York (1978)
27. P Hiemienz, *Principles of Colloid and Surface Chemistry*, M. Dekker New York (1977)
28. D Schuhmann , ed., *Propriétés électriques des interfaces chargées*, Masson, Paris (1978)
29. A Kitahara, A Watanabe, eds., *Electrical Phenomena at Interfaces: Fundamentals, Measurements, and Applications*, M. Dekker, New York (1980)
30. E J Verwey, J Th G Overbeek, *Theory and Stability of Lyophobic Colloids*, Elsevier, Amsterdam (1948)
31. B V Derjaguin, *Theory of Stability of Colloids and Thin Films*, Plenum Press, New York (1989)

32. J N Israelachvili, *Intermolecular and Surface Forces*, 2nd Ed., Academic Press, London (1991)
33. B Vincent, *Adv. Colloid Interface Sci.*, 4: 193 (1974)
34. D W Osmond, B Vincent, F A Wait, *Colloid Polymer Sci.*, 253: 676 (1975)
35. R H Ottewill, T Walker, *Kolloid-Z Polym.*, 227: 108 (1968)
36. E J Clayfield, E C Lumb, *J. Colloid Interface Sci.*, 22: 269 and 285 (1966)
37. G Hadziioannou, S Patel, S Granick, M Tirrel, *J. Am. Chem. Soc.*, 108: 2869 (1986)
38. X Zhang, R H Davis, *Fluid Mech.*, 230: 479 (1991)
39. I B Ivanov, ed., *Thin Liquid Films*, M Dekker, New York (1988)
40. K D Danov, N D Denkov, D N Petsev, I B Ivanov, R Borwankar, *Langmuir*, 9: 1731 (1993).
41. D Platikanov, ed., special issue N° 6 & 7, *J. Dispersion Sci. Technol.* vol 18 (1997)
42. R W Flumerfelt, A B Catalano, C H Tong, in *Solution Chemistry of Surfactants*, vol. 2: 571. Plenum Press, New York (1979)
43. L A Lobo, D T Wasan, in *Food Emulsions and Foams - Theory and Practice*, P J Wan, ed., A.I.Ch.E Symposium Series vol. 86, No 277 (1990)
44. D T Wasan, *Chem. Eng. Ed.*, 27, 104 (1992)
45. A Graciaa, J Lachaise, C Cucuphat, M Bourrel, J L Salager, *Langmuir*, 9: 669 and 3371 (1993)
46. P Sherman, ed., *Rheology of Emulsions*, MacMillan, New York (1963)
47. P Sherman, in *Encyclopedia of Emulsion Technology*, P Becher, ed., vol 1, M Dekker, New York (1983)
48. R Pal, E Rhodes, *J. Rheology*, 33: 1021 (1989)
49. C Bracho, Technical Report FIRP # 8302, Universidad de Los Andes, Mérida Venezuela (1983)
50. R J Farris, *Trans. Soc. Rheology*, 12: 281 (1968)
51. C Parkinson, S Matsumoto, P Sherman, *J. Colloid Interface Sci.*, 33: 150 (1970)
52. R Hoffman, *J. Rheology*, 36: 947 (1992)
53. J L Salager, M Ramirez-Gouveia, J Bullon, *Progress Colloid Polymer Sci.*, 98: 173 (1995)
54. M Ramirez-Gouveia, Technical Report FIRP # 9210, Universidad de Los Andes, Mérida Venezuela (1992)
55. H Rivas, G Nuñez, C Dalas, *Vision Tecnológica 1* :18 (1993)
56. M Z Sengun, R F Probstein, *Rheol. Acta*, 28: 382 and 394 (1989)
57. J O Hinze, *A.I.Ch.E. J.*, 1: 289 (1955)
58. R Shinnar, J M Church, *Ind. Eng. Chem.*, 52: 253 (1960)
59. F D Rumscheidt, S G Masson, *J. Colloid Interface Sci.*, 16: 210 and 238 (1961)
60. H T Chen, S Middleman, *A.I.Ch.E. J.*, 13: 989 (1967)
61. F B Sprow, *Chem. Eng. Sci.*, 22: 435 (1967)
62. H J Karam, J C Bellinger, *Ind. Eng. Chem. Fundam.*, 7: 576 (1968)
63. P Walstra, *Dechema Monograph*. 77: 87 (1974)
64. C A Coulaloglou, L L Tavlarides, *A.I.Ch.E. J.*, 22: 289 (1976)
65. K Arai, M Konno, Y Matunaga, S Saito, *J. Chem. Eng. Japan*, 10: 325 (1977)
66. J L Salager, I Loaiza-Madonado, M Miñana-Pérez, F Silva, *J. Dispersion Sci. Technol.*, 3: 279 (1982)
67. J Boyd, C Parkinson, P Sherman, *J. Colloid Interface Sci.*, 41:359 (1972)

68. K Mandani, S Friberg, *Progr. Colloid Polym. Sci.* 65: 164 (1978)
69. M Bourrel, A Graciaa, R S Schechter, W. H. Wade, *J. Colloid Interface Sci.*, 72:161 (1979)
70. J L Salager, L Quintero, E Ramos, J M Andérez, *J. Colloid Interface Sci.*, 77, 287 (1980)
71. J E Vinatieri, *Soc. Petrol. Eng. J.*, 20: 402 (1980)
72. F S Milos, D T Wasan, *Colloids Surfaces*, 4: 91 (1982)
73. R E Antón, J L Salager, *J. Colloid Interface Sci.*, 111: 54 (1986)
74. S Friberg, L Mandell, *J. Pharmaceutical Sci.*, 59: 1001 (1970)
75. R Hazzlett, R S Schechter, *Colloids Surfaces*, 29: 53 (1988)
76. A Kalbanov, H Wennerström. *Langmuir*, 12: 276 (1996)
77. J L Salager, M Miñana-Pérez, J M Andérez, J L Grosso, C I Rojas, *J. Dispersion Sci. Technol.*, 4: 161 (1983)
78. S Vijayan, C Ramachandran, H Doshi, D O Shah, 3rd Int. Conf. Surface and Colloid Science, Stockholm, Sweden, August 1979
79. J L Salager, J L Grosso, M Eslava, *Revista Técnica INTEVEP*, 2: 149 (1982)
80. K Shinoda, *Proceedings 5th Int. Congress Surface Activity*, Barcelona, Spain, vol. 2: 275 (1969)
81. J L Salager, M Pérez-Sánchez, Y Garcia, *Colloid Polym. Sci.*, 274: 81 (1996)
82. J L Salager, M Pérez-Sanchez, M Ramírez-Gouveia, J M Andérez, M I Briceño, *Récents Progrès en Génie des Procédés*, vol 11, N° 52: 123, Lavoisier, Paris (1997)
83. J L Salager, M Miñana-Pérez, M Ramírez-Gouveia, C I Rojas, *J Dispersion Sci. Technol.*, 4: 313 (1983)
84. K Shinoda, H Arai, *J. Colloid Interface Sci.*, 25: 429 (1967)
85. R E Antón, P Castillo, J L Salager, *J. Dispersion Sci. Technol.*, 7: 319 (1986)
86. E Dickinson. *Annual Reports C, The Royal Soc. of Chemistry*, p. 31. London (1986)
87. B W Brooks, H N Richmond, *Colloids Surfaces*, 58: 131 (1991)
88. H T Davis, *Colloid Surfaces A* 91: 9 (1994)
89. G J Vaessen, PhD Dissertation, Eindhoven University of Technology, Netherlands (1996)
90. P Jarry, M Miñana-Pérez, J L Salager, in "Surfactants in Solution", K Mittal, P Bothorel, eds., 6: 1689, Plenum Press New York (1987)
91. C Py, J Rouvière, Th F Tadros, M C Taelman, P Loll, *Colloids Surfaces A*, 91: 215 (1994)
92. M Pérez-Sanchez, Y Garcia, 10th International Symposium Surfactants in Solution, Caracas, Venezuela, junio 1994.
93. M Pérez-Sanchez, Technical Report #9406, Lab. FIRP Universidad de Los Andes, Mérida, Venezuela (1994)
94. A. Graciaa, J. Lachaise, J.G. Sayous, P. Grenier, S. Yiv, R.S. Schechter, and W.H. Wade, *J. Colloid Interface Sci.*, 93 (1983) 474
95. A. Graciaa, J. Lachaise, M. Bourrel, I. Osborne-Lee, R.S. Schechter, and W.H. Wade, *SPE Reservoir Eng.*, (1984) 305
96. N Márquez, R Antón, A Graciaa, J Lachaise, J L Salager, *Colloids Surfaces A*, 100: 225 (1995).
- 97.** N Márquez, R Antón, A Graciaa, J Lachaise, J L Salager, *Colloids Surfaces A*, 131: 45 (1998)
98. J L Salager, G López-Castellanos, M Miñana-Pérez, *J. Dispersion Sci. Technol.*, 11: 397 (1990)

99. A Peña, ChE Thesis, Universidad de Los Andes, Mérida, Venezuela (1996)
100. J L Salager, in *Surfactants in Solution*, A. Chattopadhyay, K. Mittal, eds., *Surfactant Science Series* vol. 64: 261, M Dekker, New York (1996).
101. F Silva, A Peña, M Miñana-Pérez, J L Salager, *Colloids Surfaces A*, 132: 221 (1998)
102. E Dickinson, *J. Colloid Interface Sci.*, 87: 416 (1982)
103. K Shinoda, H Saito, *J. Colloid Interface Sci.*, 30: 258 (1969)
104. P Becher, *J. Soc. Cosmetic Chem.*, 9: 141 (1958)
105. E Dickinson, *J. Colloid Interface Sci.*, 84: 284 (1981)
106. J L Salager, in *Surfactants in Solution*, K. Mittal, P. Bothorel, eds., vol. 4: 439, Plenum Press New York (1987)
107. J L Salager, in *Encyclopedia of Emulsion Technology*, P Becher, ed., Vol. 3: 79 (1988)
108. D H Smith, K H Lim, *Langmuir*, 6: 1071 (1990)
109. K H Lim, D H Smith, *J. Colloid Interface Sci.*, 142: 278 (1991)
110. G J Vaessen, H N Stein, *First World Congress on Emulsion*, Paris, Oct. 19-22, 1993. *Proceedings* vol. 1 paper 1-30-102
111. H Sagitani, *J. Am. Oil Chem. Soc.*, 58: 738 (1981)
112. R Pons, I Carrera, P Erra, H Kunieda, C Solans, *1st World Congress on Emulsion*, Paris october 19/22, 1993. *Proceedings*, vol. 1, paper 1-12-159.
113. B Brooks, H Richmond, *Chem. Eng. Sci.*, 49: 1053 (1994)
114. C Solans, J Esquena, N Azemar, *10th Intern. Symposium on Surfactants in Solution*, Caracas, Venezuela (1994)
115. M. Miñana-Pérez, C Gutron, C Zundel, J. M. Andérez, J L Salager, *J. Dispersion Sci. Technol.*, 20: 893 (1999)
116. J Rouviere, J L Razakarison, J Marignan, B Brun, *J. Colloid Interface Sci.*, 133: 293 (1989)
117. J Rouviere, *Information Chimie*, 325: 158 (1991)
118. M Rondón, ChE Thesis, Universidad de Los Andes, Mérida, Venezuela (1997)